Bergische Universität Wuppertal

Fakultät für Mathematik und Naturwissenschaften

Institute of Mathematical Modelling, Analysis and Computational Mathematics (IMACM)

Preprint BUW-IMACM 22/21

Maghnia Hamou Maamar, Matthias Ehrhardt, and Louiza Tabharit

A Nonstandard Finite Difference Scheme for a Time-Fractional Model of Zika Virus Transmission

November 19, 2022

http://www.imacm.uni-wuppertal.de

A Nonstandard Finite Difference Scheme for a Time-Fractional Model of Zika Virus Transmission

Maghnia Hamou Maamar, Matthias Ehrhardt, and Louiza Tabharit

This paper is dedicated in honor of Ronald E. Mickens' 80th birthday.

Abstract. In this paper we consider a compartmental model describing the transmission of Zika virus to humans and mosquito populations and an extended model including a second reservoir host of a non-human primate (monkey). This model is later generalized by a fractional time derivative.

To properly simulate the spread of the disease we design for each model a nonstandard finite difference (NSFD) scheme that is able to guarantee the positivity of the solution and exhibits the correct asymptotic behaviour of the solution.

Numerical simulations of the models illustrate these advantages, e.g. the positivity preservation, compared to using standard solver like the Runge-Kutta Fehlberg method `ode45`.

1. Introduction

The Zika virus (ZIKV) is an emerging arbovirus that is transmitted by several so-called vectors, the most important being the Aedes aegypti mosquito. Vectors are living organisms that can transmit infectious pathogens between humans, or from animals to humans. ZIKV was first isolated from a macaca monkey in the Zika forest in Uganda in 1947, giving the virus its name, cf. [**32, 33**].

The first major ZIKV epidemic began 2007 on the Yap archipelago in the Federated States of Micronesia, where a high number of cases were recorded in about 75% of the population within a few months [**36, 48**]. Later, a worldwide epidemic occurred in French Polynesia (2013-2014) with approximately 28,000 cases (about 11%) of the total population [**63**]. In 2015, ZIKV was reported in Brazil via viremic travelers or infected mosquitoes [**106**], it also began to spread in Mexico [**41**]. Messina [**72**] showed that up to 2.17 billion people live in "risk areas" (tropical and subtropical regions).

The ZIKV infection is associated with mild symptoms: Fever, headache, rash, myalgia, and conjunctivitis, similar to other arboviruses (dengue or chikungunya) [**52**] and no deaths have been reported to date. Nevertheless, ZIKV has emerged as a major cause of the development of the Guillain-Barré syndrome [**14**]. Also,

2020 *Mathematics Subject Classification.* Primary 65L05, 92D30.

Key words and phrases. nonstandard finite difference scheme, positivity, Zika virus, compartment models, time-fractional models, epidemiology, SEIR model, human-vector models.

there is still uncertainty about the outcome of co-infections with other arboviruses such as Dengue fever. Furthermore, there is no available treatment for ZIKV infection. Patient care is based on symptomatic treatment with a combination of acetaminophen and antihistamine medications [**48**].

Several mathematical models have been developed to address different categories in epidemiology, such as prediction of disease outbreaks and evaluation of control strategies [**23, 45, 64, 103**]. The first mathematical epidemic model dates back to Kermack and McKendrick (1927), who were concerned with mass events in the susceptible, infected, and remote (SIR) disease transmission cycle [**54**]. Manore and Hyman [**66**] proposed a mathematical model for ZIKV representing disease transition and population dynamics Gao [**40**] developed a model of ZIKV transmission through bites of Aedes mosquitoes and also through sexual contact. Lee and Pietz [**61**] developed a mathematical model for Zika virus using logistic growth in human populations. Nishiura et al. [**81**] proposed a mathematical Zika model that exhibits the same dynamics as Dengue fever.

In this work we derive a new *nonstandard finite difference scheme* (NSFD) for a recent SEIR (susceptible-exposed-infectious-recovered) model [**64**] that describes the spread of the Zika virus using a human-mosquito compartmental model and a human-mosquito-monkey compartmental model. Despite the fact that this NSFD scheme has a nonlinear denominator function, this schemes has a couple of favourable properties: it is explicit and due to its construction it reproduces important properties of the solution, like the number and location of fixed-points, the positivity and certain conservation laws. The goal of this work is to briefly demonstrate, in detail, how the NSFD methodology is to be applied to a system of coupled ODEs, where the discretizations are dynamical consistent with the critical properties of the continuous differential equations.

The paper is organized as follows. In Section 2, we formulate the ZIKV transmission models. Section 3 includes the stability analysis of the two considered models. In Section 4 we design the nonstandard finite difference method for the two proposed models and show how it can be extended to time-fractional variants of the models using the L1 method. In Section 5 we propose a NSFD scheme for a time-fractional version of our models. The numerical results of our novel schemes are shown in Section 6. Finally, Section 7 presents the conclusions and some outlook.

2. The ZIKV transmission models

In this section, we will briefly describe the two considered mathematical compartmental models [**64**] to describe the ZIKV transmission.

In areas without nonhuman primates, such as Yap State and French Polynesia, ZIKV is likely maintained in a human-mosquito-human cycle, suggesting that the virus has adapted to humans as reservoir hosts [**59**]. This settimng will lead us the first model, formulated in a SEIR-SEI framework.

Boorman and Porterfield [**22**] showed in a laboratory setting that Monkeys can become infected with ZIKV. However, there is no evidence that ZIKV is transmitted to humans through contact with animals. On the other hand, the presence of specific antiviral antibodies in various nonhuman primates, suggesting that other reservoirs may play a role in the ZIKV transmission cycle, cf. [**31**]. For this reason we also consider a second extended model.

2.1. The Parameters. The human population is divided into four classes (so-called 'compartments'): susceptible, exposed (latently infected), infected, and recovered (individuals who have acquired immunity). We denote the number in each compartment by S_h, E_h, I_h, and R_h. Accordingly, we divide the vector population (adult female mosquitoes) into three compartments: susceptible, exposed, and infected, with the analogous notation S_v, E_v and I_v. Next, we define the total number of populations as

$$N_h = S_h + E_h + I_h + R_h, \qquad N_v = S_v + E_v + I_v. \tag{2.1}$$

Doing so, we can consider the variables normalized to the total population

$$\begin{gathered}\mathbf{S}_h = \frac{S_h}{N_h}, \quad \mathbf{E}_h = \frac{E_h}{N_h}, \quad \mathbf{I}_h = \frac{I_h}{N_h}, \quad \mathbf{R}_h = \frac{R_h}{N_h}, \\ \mathbf{S}_v = \frac{S_v}{N_v}, \quad \mathbf{E}_v = \frac{E_v}{N_v}, \quad \mathbf{I}_h = \frac{I_v}{N_v}.\end{gathered} \tag{2.2}$$

Let us introduce a couple of parameters, cf. [**64**].

- B is the average number of bites per mosquito per day.
- β_{vh} is the probability rate that a bite from an infectious vector will infect a human, the product $B\beta_{vh}$ is the number of disease-transmitting bites per infectious mosquito per day, and the product $B\beta_{vh}I_v(t)$ is the number of disease-transmitting bites per day in the entire mosquito population at time t (measured in days). However, multiplying $B\beta_{vh}I_v(t)$ by the proportion of susceptible people at time t represents the number of disease-transmitting bites per day by infectious mosquitoes on susceptible people at time t (the daily rate at which susceptible people are exposed).
- The parameter μ_h is the proportion of the human population that dies each day ('human mortality rate').
- ν_h is the daily rate at which exposed people become infected ('human infection rate').
- η_h denotes the daily rate at which infected people become immune. ('human immunity rate').
- The parameter β_{hv} is the probability that the bite of an infectious human will infect a mosquito; $B\beta_{hv}$ is the number of disease-transmitting bites per mosquito per day. Thus, the product $B\beta_{hv}S_v(t)$ is the number of bites per day that result in disease being transmitted by susceptible mosquitoes at time t. Multiplying $B\beta_{hv}S_v(t)$ by the proportion of infectious people at time t the complete rate of disease-transmitting bites at time t (the daily rate at which susceptible mosquitoes become infected).
- The parameter μ_v is the proportion of the mosquito population that dies each day ('mosquito mortality rate').
- ν_v denotes the daily rate at which exposed mosquitoes become infected ('mosquito infection rate').

Finally, we include a constant system inflow, the birth rates Λ_h, Λ_v (e.g. birth of new individuals that can get infected, and the natural mortality rates μ_h, μ_v.

2.2. The human-mosquito model. Now we are ready to formulate the first model. The system of ordinary differential equations (ODEs) has the following form

$$
\begin{aligned}
\frac{\mathrm{d}\mathbf{S}_h(t)}{\mathrm{d}t} &= \Lambda_h - \Big(B\beta_{vh}\frac{N_v}{N_h}\,\mathbf{I}_v(t) + \mu_h\Big)\,\mathbf{S}_h(t),\\
\frac{\mathrm{d}\mathbf{E}_h(t)}{\mathrm{d}t} &= B\beta_{vh}\frac{N_v}{N_h}\,\mathbf{I}_v(t)\,\mathbf{S}_h(t) - (\nu_h + \mu_h)\mathbf{E}_h(t),\\
\frac{\mathrm{d}\mathbf{I}_h(t)}{\mathrm{d}t} &= \nu_h\mathbf{E}_h(t) - (\eta_h + \mu_h)\mathbf{I}_h(t),\\
\frac{\mathrm{d}\mathbf{R}_h(t)}{\mathrm{d}t} &= \eta_h\mathbf{I}_h(t) - \mu_h\mathbf{R}_h(t),\\
\frac{\mathrm{d}\mathbf{S}_v(t)}{\mathrm{d}t} &= \Lambda_v - (B\beta_{hv}\,\mathbf{I}_h(t) + \mu_v)\,\mathbf{S}_v(t),\\
\frac{\mathrm{d}\mathbf{E}_v(t)}{\mathrm{d}t} &= B\beta_{hv}\,\mathbf{I}_h(t)\,\mathbf{S}_v(t) - (\nu_v + \mu_v)\,\mathbf{E}_v(t),\\
\frac{\mathrm{d}\mathbf{I}_v(t)}{\mathrm{d}t} &= \nu_v\mathbf{E}_v(t) - \mu_v\mathbf{I}_v(t).
\end{aligned}
\tag{2.3}
$$

The dynamical system described by equation (2.3) is depicted in Figure 1. We note that by a convention in epidemiology models all parameters in (2.3) are assumed to be positive.

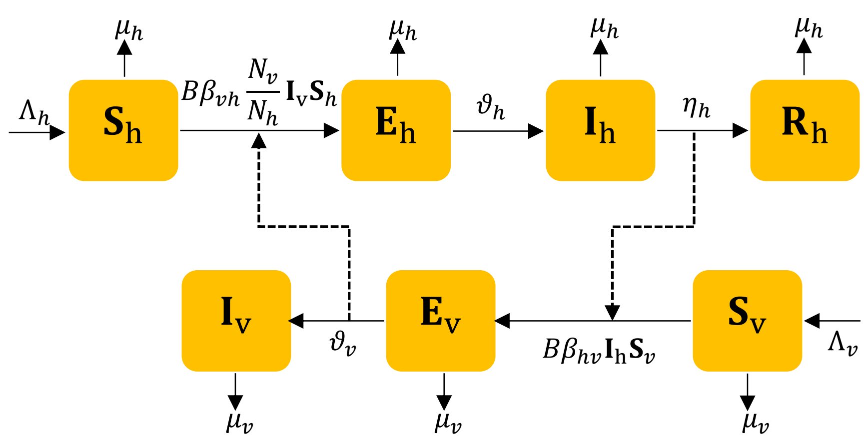

FIGURE 1. A schematic representation of the model (2.3)

Summing up the equations in (2.3) gives immediately

$$
\begin{aligned}
\frac{\mathrm{d}\mathbf{N}_h(t)}{\mathrm{d}t} &= \Lambda_h - \mu_h\,\mathbf{N}_h(t),\\
\frac{\mathrm{d}\mathbf{N}_v(t)}{\mathrm{d}t} &= \Lambda_v - \mu_v\,\mathbf{N}_v(t).
\end{aligned}
\tag{2.4}
$$

Since the Zika virus transmission has a faster dynamic than the human birthrate and the human natural mortality, $N_h(t)$ can be regarded as a conserved quantity of the above ODE system, if we set $\Lambda_h = \mu_h = 0$. This is not the case for the vector (mosquito) which has a comparable dynamic.

2.3. The human-mosquito-monkey model. Accordingly, we define the total monkey population as

$$N_m(t) = S_m(t) + E_m(t) + I_m(t) + R_m(t), \tag{2.5}$$

and introduce the normalized variables

$$\mathbf{S}_m = \frac{S_m}{N_m}, \quad \mathbf{E}_m = \frac{E_m}{N_m}, \quad \mathbf{I}_m = \frac{I_m}{N_m}, \quad \mathbf{R}_m = \frac{R_m}{N_m}. \tag{2.6}$$

Next, we introduce similar parameters for the monkey population, cf. [**64**]:

- β_{vm} is the probability rate that a bite from an infectious mosquito will infect a monkey.
- The parameter μ_m is the proportion of the monkey population that dies each day.
- ν_m is the daily rate at which exposed monkeys become infected.
- η_m the daily rate at which infected monkeys become immune.

The corresponding system of ODEs for the temporal evolution of the (normalized) human, vector and monkey population has the following form

$$\begin{aligned}
\frac{\mathrm{d}\mathbf{S}_h(t)}{\mathrm{d}t} &= \Lambda_h - \Big(B\beta_{vh}\frac{N_v}{N_h}\,\mathbf{I}_v(t) + \mu_h\Big)\,\mathbf{S}_h(t),\\
\frac{\mathrm{d}\mathbf{E}_h(t)}{\mathrm{d}t} &= B\beta_{vh}\frac{N_v}{N_h}\,\mathbf{I}_v(t)\,\mathbf{S}_h(t) - (\nu_h + \mu_h)\mathbf{E}_h(t),\\
\frac{\mathrm{d}\mathbf{I}_h(t)}{\mathrm{d}t} &= \nu_h\mathbf{E}_h(t) - (\eta_h + \mu_h)\mathbf{I}_h(t),\\
\frac{\mathrm{d}\mathbf{R}_h(t)}{\mathrm{d}t} &= \eta_h\mathbf{I}_h(t) - \mu_h\mathbf{R}_h(t),\\
\frac{\mathrm{d}\mathbf{S}_v(t)}{\mathrm{d}t} &= \Lambda_v - (B\beta_{hv}\,\mathbf{I}_h(t) + B\beta_{mv}\,\mathbf{I}_m(t) + \mu_v)\,\mathbf{S}_v(t),\\
\frac{\mathrm{d}\mathbf{E}_v(t)}{\mathrm{d}t} &= B\beta_{hv}\,\mathbf{I}_h(t)\,\mathbf{S}_v(t) + B\beta_{mv}\,\mathbf{I}_m(t)\,\mathbf{S}_v(t) - (\nu_v + \mu_v)\,\mathbf{E}_v(t),\\
\frac{\mathrm{d}\mathbf{I}_v(t)}{\mathrm{d}t} &= \nu_v\mathbf{E}_v(t) - \mu_v\mathbf{I}_v(t),\\
\frac{\mathrm{d}\mathbf{S}_m(t)}{\mathrm{d}t} &= \Lambda_m - \Big(B\beta_{vm}\frac{N_v}{N_m}\,\mathbf{I}_v(t) + \mu_m\Big)\,\mathbf{S}_m(t),\\
\frac{\mathrm{d}\mathbf{E}_m(t)}{\mathrm{d}t} &= B\beta_{vm}\frac{N_v}{N_m}\,\mathbf{I}_v(t)\,\mathbf{S}_m(t) - (\nu_m + \mu_m)\mathbf{E}_m(t),\\
\frac{\mathrm{d}\mathbf{I}_m(t)}{\mathrm{d}t} &= \nu_m\mathbf{E}_m(t) - (\eta_m + \mu_m)\mathbf{I}_m(t),\\
\frac{\mathrm{d}\mathbf{R}_m(t)}{\mathrm{d}t} &= \eta_m\mathbf{I}_m(t) - \mu_m\mathbf{R}_m(t).
\end{aligned} \tag{2.7}$$

The dynamical system described by equations (2.7) is depicted in Figure 2.

Again, summing up the equations in (2.7) yields for the total populations

$$\begin{aligned}
\frac{\mathrm{d}\mathbf{N}_h(t)}{\mathrm{d}t} &= \Lambda_h - \mu_h\,\mathbf{N}_h(t),\\
\frac{\mathrm{d}\mathbf{N}_v(t)}{\mathrm{d}t} &= \Lambda_v - \mu_v\,\mathbf{N}_v(t),\\
\frac{\mathrm{d}\mathbf{N}_m(t)}{\mathrm{d}t} &= \Lambda_m - \mu_m\,\mathbf{N}_m(t).
\end{aligned} \tag{2.8}$$

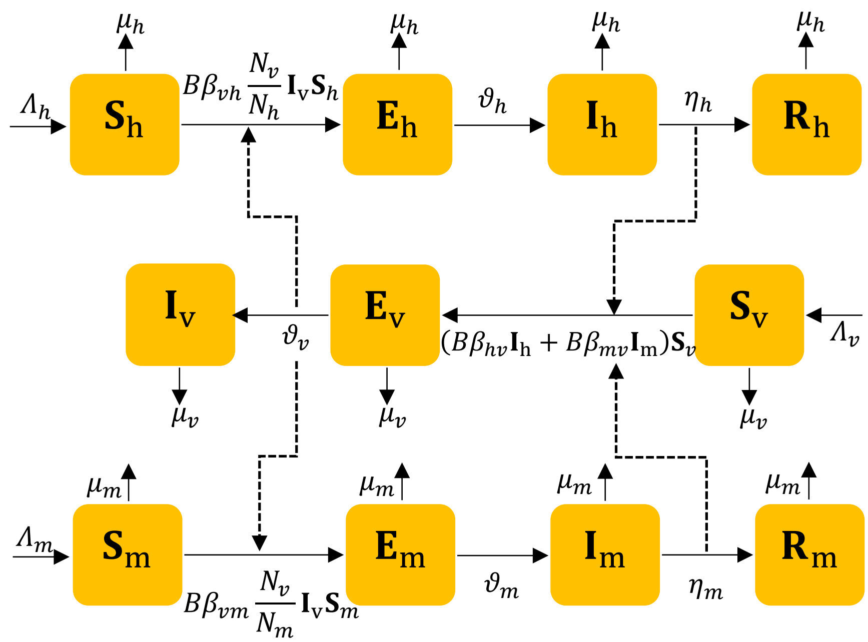

FIGURE 2. A schematic representation of the model (2.7).

and analogously, $N_h(t)$ and $N_m(t)$ can be regarded as a conserved quantity of the above ODE system, if we set $\Lambda_h = \mu_h = 0$ and $\Lambda_m = \mu_m = 0$.

3. Stability Analysis

In this section we will briefly review the results from [**64**] and add new findings that are used later in the numerical part. First, we investigate the existence and stability of the equilibrium points of system (2.3), i.e. the steady state points.

Using the following relationships for the normalized populations (2.2),

$$\mathbf{R}_h(t) = 1 - \mathbf{S}_h(t) - \mathbf{E}_h(t) - \mathbf{I}_h(t), \qquad \mathbf{S}_v(t) = 1 - \mathbf{E}_v(t) - \mathbf{I}_v(t), \tag{3.1}$$

and setting $\Lambda_h = \mu_h$ (since the human dynamics is much slower than the one of the mosquitos), we obtain from system (2.3) an equivalent reduced system with only 5 components

(3.2)
$$\begin{aligned}
\frac{\mathrm{d}\mathbf{S}_h(t)}{\mathrm{d}t} &= \mu_h - \mu_h \mathbf{S}_h(t) - pB\beta_{vh}\,\mathbf{I}_v(t)\,\mathbf{S}_h(t),\\
\frac{\mathrm{d}\mathbf{E}_h(t)}{\mathrm{d}t} &= -(\nu_h + \mu_h)\,\mathbf{E}_h(t) + pB\beta_{vh}\,\mathbf{I}_v(t)\,\mathbf{S}_h(t),\\
\frac{\mathrm{d}\mathbf{I}_h(t)}{\mathrm{d}t} &= \nu_h \mathbf{E}_h(t) - (\eta_h + \mu_h)\,\mathbf{I}_h(t),\\
\frac{\mathrm{d}\mathbf{E}_v(t)}{\mathrm{d}t} &= B\beta_{hv}\,\mathbf{I}_h(t) - (\nu_v + \mu_v)\,\mathbf{E}_v(t) - B\beta_{hv}\,\mathbf{I}_h(t)\,\mathbf{E}_v(t) - B\beta_{hv}\,\mathbf{I}_h(t)\mathbf{I}_v(t),\\
\frac{\mathrm{d}\mathbf{I}_v(t)}{\mathrm{d}t} &= \nu_v \mathbf{E}_v(t) - \mu_v \mathbf{I}_v(t),
\end{aligned}$$

where we have used the abbreviation (and assumption)

$$p = \frac{N_v}{N_h} > 1. \tag{3.3}$$

The system (3.2) has the Jacobi matrix $J = J(\mathbf{S}_h, \mathbf{E}_h, \mathbf{I}_h, \mathbf{E}_v, \mathbf{I}_v)$ given by

$$\begin{pmatrix}
-\mu_h - pB\beta_{vh}\mathbf{I}_v & 0 & 0 & 0 & -pB\beta_{vh}\mathbf{S}_h\\
pB\beta_{vh}\mathbf{I}_v & -(\nu_h+\mu_h) & 0 & 0 & pB\beta_{vh}\mathbf{S}_h\\
0 & \nu_h & -(\eta_h+\mu_h) & 0 & 0\\
0 & 0 & B\beta_{hv}(1-\mathbf{E}_v-\mathbf{I}_v) & -(\nu_v+\mu_v) - B\beta_{hv}\mathbf{I}_h & -B\beta_{hv}\mathbf{I}_h\\
0 & 0 & 0 & \nu_v & -\mu_v
\end{pmatrix}.$$

3.1. Equilibrium Points. In [**64**] the basic reproduction number R_0 of the reduced system (3.2) was determined as

$$R_0 = \frac{\nu_v \nu_h p B^2 \beta_{hv}\beta_{vh}}{\mu_v(\nu_v+\mu_v)(\eta_h+\mu_h)(\nu_h+\mu_h)}. \tag{3.4}$$

Further, it was shown that the system (3.2) has always the *disease free equilibrium* (DFE)

$$(\mathbf{S}_h^*, \mathbf{E}_h^*, \mathbf{I}_h^*, \mathbf{E}_v^*, \mathbf{I}_v^*) = (1,0,0,0,0),$$

which is the unique equilibrium point in the case $R_0 \le 1$.

For $R_0 > 1$ the system (3.2) has a second stationary point, the *endemic equilibrium* (EE), given by, cf. [**64**]

$$\begin{aligned}
\mathbf{S}_h^{**} &= \frac{p\nu_v B\beta_{vh} + \mu_h(\nu_v+\mu_v)R_0}{\big(\nu_v pB\beta_{vh} + \mu_h(\nu_v+\mu_v)\big)R_0},\\
\mathbf{E}_h^{**} &= \frac{\nu_v\mu_h pB\beta_{vh}}{\nu_h+\mu_h}\,\frac{R_0-1}{\big(\nu_v pB\beta_{vh} + \mu_h(\nu_v+\mu_v)\big)R_0},\\
\mathbf{I}_h^{**} &= \frac{\mu_h\nu_v\nu_h pB\beta_{vh}}{(\eta_h+\mu_h)(\nu_h+\mu_h)}\,\frac{R_0-1}{\big(\nu_v pB\beta_{vh} + \mu_h(\nu_v+\mu_v)\big)R_0},\\
\mathbf{E}_v^{**} &= \frac{\mu_v\mu_h(R_0-1)}{\big(\nu_v pB\beta_{vh} + \mu_h(\nu_v+\mu_v)\big)R_0},\\
\mathbf{I}_v^{**} &= \frac{\nu_v\mu_h(R_0-1)}{\big(\nu_v pB\beta_{vh} + \mu_h(\nu_v+\mu_v)\big)R_0}.
\end{aligned} \tag{3.5}$$

Evaluating the Jacobian matrix J of the system (3.2) at the DFE, one obtains

$$J(\mathrm{DFE}) = \begin{pmatrix} -\mu_h & 0 & 0 & 0 & -pB\beta_{vh} \\ 0 & -(\nu_h+\mu_h) & 0 & 0 & pB\beta_{vh} \\ 0 & \nu_h & -(\eta_h+\mu_h) & 0 & 0 \\ 0 & 0 & B\beta_{hv} & -(\nu_v+\mu_v) & 0 \\ 0 & 0 & 0 & \nu_v & -\mu_v \end{pmatrix}.$$

In [**64**] it was shown that all eigenvalues of this matrix have negative real parts, i.e. the DFE of the reduced system (3.2) is *locally asymptotically stable*.

Similarly, the Jacobian matrix can be evaluated at the EE and one can prove that for $R_0 > 1$, the EE of the system (3.2) is *locally asymptotically stable*, cf. [**64**].

4. The Nonstandard Finite Difference Method

In this section we explain the technique of nonstandard finite difference schemes (NSFDs). A NSFD scheme is constructed to satisfy the positivity condition and the conservation laws. Consequently, the solutions are bounded, i.e. stable. Also, only the fixed-points of the ODE systems (2.3), (2.7) appear in the NSFD scheme. The specific full details are not given; we refer to the book of Mickens [**73**] for the discretization strategy.

4.1. Nonstandard Finite Difference Schemes. NSFD methods for the numerical integration of differential equations had their origin in a paper by Mickens published in 1989 [**73**]. In this section, an NSFD scheme is constructed to satisfy the essential positivity condition and the conservation law for $\Lambda_h = \mu_h = 0$, $\Lambda_v = \mu_v = 0$ and $\Lambda_m = \mu_m = 0$ which leads as a byproduct to the stability of the scheme. We will also check that the equilibrium points of the ODE model also appear in the proposed NSFD scheme.

Let us recall that schemes such as those based on Runge-Kutta methods can yield wrong negative solutions (see [**71, 42**]) can produce 'false' or 'spurious' fixed-points, which are not fixed points of the original ODE system, cf. [**74**].

Finally, we will determine in Section 4.4 the so-called denominator function $\phi(h)$, such that we obtain the correct long-time behaviour. We refer to [**16, 100**], where we established an NSFD scheme for a similar compartment model as here.

We remind the reader that a numerical scheme for a system of first-order differential equations is called *NSFD scheme* if at least one of the following conditions [**73**] is satisfied:

- The orders of the discrete derivatives should be equal to the orders of the corresponding derivatives appearing in the differential equations.
- Discrete representations for derivatives must, in general, have nontrivial denominator functions. Here, the first-order derivatives in the system are approximated by the generalized forward difference method (forward Euler method) $\frac{\mathrm{d}u^n}{\mathrm{d}t} \approx \frac{u^{n+1}-u^n}{\phi(h)}$, where $u^n \approx u(t_n)$ and $\phi \equiv \phi(h) > 0$ is the so-called *denominator function* such that $\phi(h) = h + \mathcal{O}(h^2)$, with h the step size. This function $\phi(h)$ is chosen so that the discrete solution has the same asymptotic behaviour as the analytical solution.
- The nonlinear terms are approximated by non-local discrete representations, for instance by a suitable function of several points of a mesh, like $u^2(t_n) \approx u^n u^{n+1}$ or $u^3(t_n) \approx (u^n)^2 u^{n+1}$.

- Special conditions that hold for either the ODE and/or its solutions should also apply to the difference equation model and/or its solution, e.g. positivity of the solution, convexity of the solution (in finance), equilibrium points of the ODE system, including their local asymptotic stability properties.

In NSFD schemes, derivatives must be modeled by discrete analogues that take the form, cf. [**73**]

$$\frac{\mathrm{d}u(t)}{\mathrm{d}t} \to \frac{u^{n+1} - \psi(h)u^n}{\phi(h)}\,, \tag{4.1}$$

where $t_n = n\,h$, u^n is the approximation of $u(t_n)$, and $\psi(h) = 1+\mathcal{O}(h)$. The purpose of this more general time discretization (4.1) in NSFD schemes, is to properly model the asymptotic long-time behaviour of the solution.

4.2. NSFD scheme for the human-mosquito model. Next, we propose the following NSFD discretization for solving the ODE system (2.3)

$$\begin{aligned}
\frac{\mathbf{S}_h^{n+1} - \mathbf{S}_h^n}{\phi(h)} &= \Lambda_h - \Big(B\beta_{vh}\frac{N_v}{N_h}\,\mathbf{I}_v^n + \mu_h\Big)\,\mathbf{S}_h^{n+1},\\
\frac{\mathbf{E}_h^{n+1} - \mathbf{E}_h^n}{\phi(h)} &= B\beta_{vh}\frac{N_v}{N_h}\,\mathbf{I}_v^n\,\mathbf{S}_h^{n+1} - (\nu_h + \mu_h)\mathbf{E}_h^{n+1},\\
\frac{\mathbf{I}_h^{n+1} - \mathbf{I}_h^n}{\phi(h)} &= \nu_h\mathbf{E}_h^{n+1} - (\eta_h + \mu_h)\mathbf{I}_h^{n+1},\\
\frac{\mathbf{R}_h^{n+1} - \mathbf{R}_h^n}{\phi(h)} &= \eta_h\mathbf{I}_h^{n+1} - \mu_h\mathbf{R}_h^{n+1},\\
\frac{\mathbf{S}_v^{n+1} - \mathbf{S}_v^n}{\phi(h)} &= \Lambda_v - (B\beta_{hv}\,\mathbf{I}_h^{n+1} + \mu_v)\,\mathbf{S}_v^{n+1},\\
\frac{\mathbf{E}_v^{n+1} - \mathbf{E}_v^n}{\phi(h)} &= B\beta_{hv}\,\mathbf{I}_h^{n+1}\,\mathbf{S}_v^{n+1} - (\nu_v + \mu_v)\,\mathbf{E}_v^{n+1},\\
\frac{\mathbf{I}_v^{n+1} - \mathbf{I}_v^n}{\phi(h)} &= \nu_v\mathbf{E}_v^{n+1} - \mu_v\mathbf{I}_v^{n+1},
\end{aligned} \tag{4.2}$$

with a denominator function $\phi(h)$ to be determined later, given by (4.12).

Let us briefly comment on the discretizations of the nonlinear (here: quadratic) terms. For example, in the first line (4.2) we have discretized the nonlinear contact term $\beta_{vh}I_v(t)S_h(t)$ in (2.3) by $\beta_{vh}I_v^nS_h^{n+1}$ rather than, say, $I_v^nS_h^n$ or $I_v^{n+1}S_h^{n+1}$. The rule is that exactly one factor of the variable appearing in the time derivative (here S_h) must be taken at the new time level $n+1$. This is needed to obtain a positivity preserving scheme, see (4.3). In order not to destroy the explicit sequential evaluation, all other variables are taken from the previous time level, unless they are already known from a previous step, like $I_h^{n+1}S_v^{n+1}$ in the fifth line. If possible, discrete conservation properties (here: total population of humans, vectors) must also be taken into account.

Observe that although the initial scheme (4.2) can be considered implicit, the variables at the $(n+1)$-th discrete-time level can be explicitly calculated in terms of the previously known variable values as given in the sequence of the equations above, i.e. we can rewrite it as an explicit form

$$
\begin{aligned}
\mathbf{S}_h^{n+1} &= \frac{\mathbf{S}_h^n + \phi(h)\,\Lambda_h}{1+\phi(h)\left(B\beta_{vh}\frac{N_v}{N_h}\,\mathbf{I}_v^n + \mu_h\right)},\\
\mathbf{E}_h^{n+1} &= \frac{\mathbf{E}_h^n + \phi(h)\,B\beta_{vh}\frac{N_v}{N_h}\,\mathbf{I}_v^n\,\mathbf{S}_h^{n+1}}{1+\phi(h)\,(\nu_h+\mu_h)},\\
\mathbf{I}_h^{n+1} &= \frac{\mathbf{I}_h^n + \phi(h)\,\nu_h\mathbf{E}_h^{n+1}}{1+\phi(h)\,(\eta_h+\mu_h)},\\
\mathbf{R}_h^{n+1} &= \frac{\mathbf{R}_h^n + \phi(h)\,\eta_h\mathbf{I}_h^{n+1}}{1+\phi(h)\,\mu_h},\\
\mathbf{S}_v^{n+1} &= \frac{\mathbf{S}_v^n + \phi(h)\,\Lambda_v}{1+\phi(h)\left(B\beta_{hv}\,\mathbf{I}_h^{n+1} + \mu_v\right)},\\
\mathbf{E}_v^{n+1} &= \frac{\mathbf{E}_v^n + \phi(h)\,B\beta_{hv}\,\mathbf{I}_h^{n+1}\,\mathbf{S}_v^{n+1}}{1+\phi(h)\,(\nu_v+\mu_v)},\\
\mathbf{I}_v^{n+1} &= \frac{\mathbf{I}_v^n + \phi(h)\,\nu_v\mathbf{E}_v^{n+1}}{1+\phi(h)\,\mu_v}.
\end{aligned}
\tag{4.3}
$$

The calculation must be done in exactly this order. All parameters appearing in these type of epidemic models are always non-negative. This is the convention used in fields related to the spread of diseases. From the explicit representation (4.2) it is easy to deduce that this scheme preserves the positivity, given some natural conditions on the parameters.

4.3. NSFD scheme for the human-mosquito-monkey model. Correspondingly, the NSFD discretization for solving the ODE system (2.7) reads

$$
\begin{aligned}
\frac{\mathbf{S}_h^{n+1}-\mathbf{S}_h^n}{\phi(h)} &= \Lambda_h - \left(B\beta_{vh}\frac{N_v}{N_h}\,\mathbf{I}_v^n + \mu_h\right)\mathbf{S}_h^{n+1},\\
\frac{\mathbf{E}_h^{n+1}-\mathbf{E}_h^n}{\phi(h)} &= B\beta_{vh}\frac{N_v}{N_h}\,\mathbf{I}_v^n\,\mathbf{S}_h^{n+1} - (\nu_h+\mu_h)\mathbf{E}_h^{n+1},\\
\frac{\mathbf{I}_h^{n+1}-\mathbf{I}_h^n}{\phi(h)} &= \nu_h\mathbf{E}_h^{n+1} - (\eta_h+\mu_h)\mathbf{I}_h^{n+1},\\
\frac{\mathbf{R}_h^{n+1}-\mathbf{R}_h^n}{\phi(h)} &= \eta_h\mathbf{I}_h^{n+1} - \mu_h\mathbf{R}_h^{n+1},\\
\frac{\mathbf{S}_v^{n+1}-\mathbf{S}_v^n}{\phi(h)} &= \Lambda_v - (B\beta_{hv}\,\mathbf{I}_h^{n+1} + B\beta_{mv}\,\mathbf{I}_m^{n+1} + \mu_v)\,\mathbf{S}_v^{n+1},\\
\frac{\mathbf{E}_v^{n+1}-\mathbf{E}_v^n}{\phi(h)} &= B\beta_{hv}\,\mathbf{I}_h^{n+1}\,\mathbf{S}_v^{n+1} + B\beta_{mv}\,\mathbf{I}_m^{n+1}\,\mathbf{S}_v^{n+1} - (\nu_v+\mu_v)\,\mathbf{E}_v^{n+1},\\
\frac{\mathbf{I}_v^{n+1}-\mathbf{I}_v^n}{\phi(h)} &= \nu_v\mathbf{E}_v^{n+1} - \mu_v\mathbf{I}_v^{n+1}\\
\frac{\mathbf{S}_m^{n+1}-\mathbf{S}_m^n}{\phi(h)} &= \Lambda_m - \left(B\beta_{vm}\frac{N_v}{N_m}\,\mathbf{I}_v^{n+1} + \mu_m\right)\mathbf{S}_m^{n+1},\\
\frac{\mathbf{E}_m^{n+1}-\mathbf{E}_m^n}{\phi(h)} &= B\beta_{vm}\frac{N_v}{N_m}\,\mathbf{I}_v^{n+1}\,\mathbf{S}_m^{n+1} - (\nu_m+\mu_m)\mathbf{E}_m^{n+1},
\end{aligned}
\tag{4.4}
$$

$$\frac{\mathbf{I}_m^{n+1}-\mathbf{I}_m^n}{\phi(h)} = \nu_m \mathbf{E}_m^{n+1} - (\eta_m+\mu_m)\mathbf{I}_m^{n+1},$$
$$\frac{\mathbf{R}_m^{n+1}-\mathbf{R}_m^n}{\phi(h)} = \eta_m \mathbf{I}_m^{n+1} - \mu_m \mathbf{R}_m^{n+1}.$$

$$\begin{aligned}
\mathbf{S}_h^{n+1} &= \frac{\mathbf{S}_h^n + \phi(h)\,\Lambda_h}{1+\phi(h)\left(B\beta_{vh}\frac{N_v}{N_h}\,\mathbf{I}_v^n + \mu_h\right)},\\
\mathbf{E}_h^{n+1} &= \frac{\mathbf{E}_h^n + \phi(h)\,B\beta_{vh}\frac{N_v}{N_h}\,\mathbf{I}_v^n\,\mathbf{S}_h^{n+1}}{1+\phi(h)\,(\nu_h+\mu_h)},\\
\mathbf{I}_h^{n+1} &= \frac{\mathbf{I}_h^n + \phi(h)\,\nu_h \mathbf{E}_h^{n+1}}{1+\phi(h)\,(\eta_h+\mu_h)},\\
\mathbf{R}_h^{n+1} &= \frac{\mathbf{R}_h^n + \phi(h)\,\eta_h \mathbf{I}_h^{n+1}}{1+\phi(h)\,\mu_h},\\
\mathbf{S}_v^{n+1} &= \frac{\mathbf{S}_v^n + \phi(h)\,\Lambda_v}{1+\phi(h)\left(B\beta_{hv}\,\mathbf{I}_h^{n+1} + B\beta_{mv}\,\mathbf{I}_m^{n+1} + \mu_v\right)},\\
\mathbf{E}_v^{n+1} &= \frac{\mathbf{E}_v^n + \phi(h)\left(B\beta_{hv}\,\mathbf{I}_h^{n+1} + B\beta_{mv}\,\mathbf{I}_m^{n+1}\right)\mathbf{S}_v^{n+1}}{1+\phi(h)\,(\nu_v+\mu_v)},\\
\mathbf{I}_v^{n+1} &= \frac{\mathbf{I}_v^n + \phi(h)\,\nu_v \mathbf{E}_v^{n+1}}{1+\phi(h)\,\mu_v},\\
\mathbf{S}_m^{n+1} &= \frac{\mathbf{S}_m^n + \phi(h)\,\Lambda_m}{1+\phi(h)\left(B\beta_{vm}\frac{N_v}{N_m}\,\mathbf{I}_v^{n+1} + \mu_m\right)},\\
\mathbf{E}_m^{n+1} &= \frac{\mathbf{E}_m^n + \phi(h)\,B\beta_{vm}\frac{N_v}{N_m}\,\mathbf{I}_v^{n+1}\,\mathbf{S}_m^{n+1}}{1+\phi(h)\,(\nu_m+\mu_m)},\\
\mathbf{I}_m^{n+1} &= \frac{\mathbf{I}_m^n + \phi(h)\,\nu_m \mathbf{E}_m^{n+1}}{1+\phi(h)\,(\eta_m+\mu_m)},\\
\mathbf{R}_m^{n+1} &= \frac{\mathbf{R}_m^n + \phi(h)\,\eta_m \mathbf{I}_m^{n+1}}{1+\phi(h)\,\mu_m}.
\end{aligned} \tag{4.5}$$

4.4. The denominator function. Finally, it only remains to correctly determine the denominator function $\phi(h)$. To do so, we reconsider the combined total population $N = N_h + N_v$ of the ODE system (2.3) (or $N = N_h + N_v + N_m$) for system (2.7)), now without neglecting the birthrates and the natural mortality. Here, we introduce accordingly the combined values $\Lambda = \Lambda_h + \Lambda_v$, $\mu = \mu_h + \mu_v$ for system (2.3) and $\Lambda = \Lambda_h + \Lambda_v + \Lambda_m$, $\mu = \mu_h + \mu_v + \mu_m$ for the extended system (2.7).

Adding the equations of (2.3) or (2.7), we easily obtain the following differential equation describing the dynamics of the combined total population N

$$\frac{\mathrm{d}N(t)}{\mathrm{d}t} = \Lambda - \mu\,N(t)\,. \tag{4.6}$$

It is solved by

$$N(t) = \frac{\Lambda}{\mu} + \left(N(0) - \frac{\Lambda}{\mu}\right)e^{-\mu t} = N(0) + \left(N(0) - \frac{\Lambda}{\mu}\right)(e^{-\mu t} - 1), \tag{4.7}$$

with $N(0) = N_h(0) + N_v(0) + N_m(0)$. From (4.7) we immediately deduce that we have in the long term $\lim_{t\to\infty} N(t) = \Lambda/\mu$. Let us briefly note that this link between the transient dynamics and their 'natural' limiting systems can be used to reduce the dimension of this model, cf. [**27**].

Next, adding the equations in the discrete NSFD model (4.2) yields

$$\frac{N^{n+1}-N^n}{\phi(h)} = \Lambda - \mu\, N^{n+1}, \tag{4.8}$$

i.e.

$$\begin{aligned} N^{n+1} &= \frac{N^n+\phi(h)\Lambda}{1+\phi(h)\,\mu} = N^n - \Bigl(N^n - \frac{\Lambda}{\mu}\Bigr)\frac{\phi(h)\,\mu}{1+\phi(h)\,\mu} \\ &= N^n + \Bigl(N^n - \frac{\Lambda}{\mu}\Bigr)\Bigl(\frac{1}{1+\phi(h)\,\mu} - 1\Bigr). \end{aligned} \tag{4.9}$$

The denominator function can be derived by comparing Equation (4.8) with the discrete version of Equation (4.7), that is

$$N^{n+1} = N^n + \Bigl(N^n - \frac{\Lambda}{\mu}\Bigr)\,(e^{-\mu h}-1), \quad h=\Delta t, \tag{4.10}$$

such that the (positive) denominator function is defined by

$$\frac{1}{1+\phi(h)\,\mu} = e^{-\mu h}, \tag{4.11}$$

i.e.

$$\phi(h) = \frac{e^{\mu h}-1}{\mu} = \frac{1+\mu h + \frac{1}{2}\mu^2 h^2 + \ldots - 1}{\mu} = h + \frac{\mu h^2}{2} + \ldots = h + \mathcal{O}(h^2). \tag{4.12}$$

Note that the conservation property requires all the denominator functions $\phi(h)$ for the compartments to be the same. Otherwise, it would be impossible to obtain a discrete analogue like (4.8) which is also needed for stability reasons.

Remark 4.1. An even more accurate way to compute the denominator function would take into account the transition rate Υ_i at which the i^{th} compartment is entered by individuals for all model compartments $\mathcal{K}_i$, $i=1,2,\ldots$ (e.g. β_{vh}, ν_h, η_h, $\nu_v, \ldots$), cf. [**37**]. In this case the parameter μ occurring in the denominator function in Equation (4.12) would be replaced by a parameter $1/T^*$. T^* could be determined as the minimum of the inverse transition parameters:

$$T^* = \min_{i=1,2,\ldots}\Bigl\{\frac{1}{\Upsilon_i}\Bigr\}.$$

5. A NSFD scheme for a time-fractional model

The fractional-order dynamics of the transmission of the Zika virus to human and vector populations is given, as a generalization of model (2.3), by the following system

$$
\begin{aligned}
{}^{C}D^{\alpha}\mathbf{S}_h(t) &= \Lambda_h^{\alpha} - \Big(B^{\alpha}\beta_{vh}\frac{N_v}{N_h}\mathbf{I}_v(t) + \mu_h^{\alpha}\Big)\mathbf{S}_h(t),\\
{}^{C}D^{\alpha}\mathbf{E}_h(t) &= B^{\alpha}\beta_{vh}\frac{N_v}{N_h}\mathbf{I}_v(t)\mathbf{S}_h(t) - (\nu_h^{\alpha} + \mu_h^{\alpha})\mathbf{E}_h(t),\\
{}^{C}D^{\alpha}\mathbf{I}_h(t) &= \nu_h^{\alpha}\mathbf{E}_h(t) - (\eta_h^{\alpha} + \mu_h^{\alpha})\mathbf{I}_h(t),\\
{}^{C}D^{\alpha}\mathbf{R}_h(t) &= \eta_h^{\alpha}\mathbf{I}_h(t) - \mu_h^{\alpha}\mathbf{R}_h(t),\\
{}^{C}D^{\alpha}\mathbf{S}_v(t) &= \Lambda_v^{\alpha} - (B^{\alpha}\beta_{hv}\mathbf{I}_h(t) + \mu_v^{\alpha})\mathbf{S}_v(t),\\
{}^{C}D^{\alpha}\mathbf{E}_v(t) &= B^{\alpha}\beta_{hv}\mathbf{I}_h(t)\mathbf{S}_v(t) - (\nu_v^{\alpha} + \mu_v^{\alpha})\mathbf{E}_v(t),\\
{}^{C}D^{\alpha}\mathbf{I}_v(t) &= \nu_v^{\alpha}\mathbf{E}_v(t) - \mu_v^{\alpha}\mathbf{I}_v(t),
\end{aligned} \tag{5.1}
$$

with the initial conditions

$$\mathbf{S}_h(0),\ \mathbf{E}_h(0),\ \mathbf{I}_h(0),\ \mathbf{R}_h(0),\ \mathbf{S}_v(0),\ \mathbf{E}_v(0),\ \mathbf{I}_v(0) \geq 0,$$

where ${}^{C}D^{\alpha}X(t)$ denotes the Caputo derivative and it is defined as:

$${}^{C}D^{\alpha}X(t) = \frac{1}{\Gamma(1-\alpha)}\int_0^t \frac{dX(\tau)}{d\tau}(t-\tau)^{-\alpha}d\tau, \quad t > 0 \text{ and } 0 < \alpha < 1.$$

Adding the equations of the system (5.1) yields

$${}^{C}D^{\alpha}\mathbf{N}(t) = \Lambda^{\alpha} - \mu^{\alpha}\mathbf{N}(t), \tag{5.2}$$

where $\Lambda^{\alpha} = \Lambda_h^{\alpha} + \Lambda_v^{\alpha}$ and $\mu^{\alpha} = \mu_h^{\alpha} + \mu_v^{\alpha}$.

In the model (5.1) given above, we modified the right-hand sides parameters μ_h^{α}, B^{α}, ν_h^{α}, η_h^{α}, μ_v^{α} and ν_v^{α} using the procedure described in Diethelm [**35**] in order to adjust the dimensions because the dimension of the left-hand sides of the equations is $(\text{time})^{-\alpha}$. Note that in the limiting case $\alpha \to 1$, the system (5.1) reduces to the classical system given in (2.3).

Let $t_0 = 0 < t_1 < \cdots < t_N = T$, $t_n = nT/N$, where $N \in \mathbb{N}$. Next, we present a numerical approximation of the Caputo derivative using the NSFD method. We have

$${}^{C}D^{\alpha}X(t)\Big|_{t=t_{n+1}} = \frac{1}{\Gamma(1-\alpha)}\sum_{j=0}^{n}\int_{t_j}^{t_{j+1}} \frac{dX(\tau)}{d\tau}(t_{n+1}-\tau)^{-\alpha}d\tau$$

We discretize the term $\frac{dX(\tau)}{d\tau}$ on $[t_j, t_{j+1}]$ as

$$\frac{dX(\tau)}{d\tau} = \frac{X^{j+1} - X^j}{\phi(h)},$$

where $X^j = X(t_j)$ and $\phi(h)$ from (4.12).

$${}^{C}D^{\alpha}X(t)\Big|_{t=t_{n+1}} \approx \frac{1}{\Gamma(2-\alpha)}\sum_{j=0}^{n}\Delta_{\alpha,n}^{j}\frac{X^{j+1} - X^j}{\phi(h)},$$

where

$$\Delta_{\alpha,n}^{j} = \big((t_{n+1} - t_j)^{1-\alpha} - (t_{n+1} - t_{j+1})^{1-\alpha}\big).$$

Each equation in (5.1) can be written as

$${}^{C}D^{\alpha}X(t) = F\big(X(t)\big),$$

at the point $t = t_{n+1}$, we have

$$\frac{1}{\Gamma(2-\alpha)} \sum_{j=0}^{n} \Delta_{\alpha,n}^{j} \frac{X^{j+1} - X^{j}}{\phi(h)} - F(X^{n+1}) = 0, \quad n = 1, \ldots, N-1. \tag{5.3}$$

Now, we apply the scheme (5.3) to the system (2.3), we obtain

$$\begin{aligned}
\mathbf{S}_h^{n+1} &= \frac{h^{1-\alpha}\mathbf{S}_h^n - \sum_{j=0}^{n-1} \Delta_{\alpha,n}^{j}(\mathbf{S}_h^{j+1} - \mathbf{S}_h^{j}) + \Gamma(2-\alpha)\phi(h)\mu_h^\alpha}{\Big(h^{1-\alpha} + \Gamma(2-\alpha)\phi(h)\Big(B^\alpha \beta_{vh}\dfrac{N_v}{N_h}\mathbf{I}_v^n + \mu_h^\alpha\Big)\Big)}, \\
\mathbf{E}_h^{n+1} &= \frac{h^{1-\alpha}\mathbf{E}_h^n - \sum_{j=0}^{n-1} \Delta_{\alpha,n}^{j}(\mathbf{E}_h^{j+1} - \mathbf{E}_h^{j}) + \Gamma(2-\alpha)\phi(h)B^\alpha\beta_{vh}\dfrac{N_v}{N_h}\mathbf{I}_v^n\mathbf{S}_h^{n+1}}{\big(h^{1-\alpha} + \Gamma(2-\alpha)\phi(h)(\nu_h^\alpha + \mu_h^\alpha)\big)}, \\
\mathbf{I}_h^{n+1} &= \frac{h^{1-\alpha}\mathbf{I}_h^n - \sum_{j=0}^{n-1} \Delta_{\alpha,n}^{j}(\mathbf{I}_h^{j+1} - \mathbf{I}_h^{j}) + \Gamma(2-\alpha)\phi(h)\nu_h^\alpha\mathbf{E}_h^{n+1}}{\big(h^{1-\alpha} + \Gamma(2-\alpha)\phi(h)(\eta_h^\alpha + \mu_h^\alpha)\big)}, \\
\mathbf{R}_h^{n+1} &= \frac{h^{1-\alpha}\mathbf{R}_h^n - \sum_{j=0}^{n-1} \Delta_{\alpha,n}^{j}(\mathbf{R}_h^{j+1} - \mathbf{R}_h^{j}) + \phi(h)\Gamma(2-\alpha)\eta_h^\alpha\mathbf{I}_h^{n+1}}{\big(h^{1-\alpha} + \phi(h)\Gamma(2-\alpha)\mu_h^\alpha\big)}, \\
\mathbf{S}_v^{n+1} &= \frac{h^{1-\alpha}\mathbf{S}_v^j - \sum_{j=0}^{n-1} \Delta_{\alpha,n}^{j}(\mathbf{S}_v^{j+1} - \mathbf{S}_v^{j}) + \Gamma(2-\alpha)\mu_v^\alpha}{\big(h^{1-\alpha} + \phi(h)\Gamma(2-\alpha)(B^\alpha\beta_{hv}\mathbf{I}_h^{n+1} + \mu_v^\alpha)\big)}, \\
\mathbf{E}_v^{n+1} &= \frac{h^{1-\alpha}\mathbf{E}_v^n - \sum_{j=0}^{n} \Delta_{\alpha,n}^{j}(\mathbf{E}_v^{j+1} - \mathbf{E}_v^{j}) + \phi(h)\Gamma(2-\alpha)B^\alpha\beta_{hv}\mathbf{I}_h^{n+1}\mathbf{S}_v^{n+1}}{\big(h^{1-\alpha} + \phi(h)\Gamma(2-\alpha)(\nu_v^\alpha + \mu_v^\alpha)\big)}, \\
\mathbf{I}_v^{n+1} &= \frac{h^{1-\alpha}\mathbf{I}_v^n - \sum_{j=0}^{n-1} \Delta_{\alpha,n}^{j}(\mathbf{I}_v^{j+1} - \mathbf{I}_v^{j}) + \phi(h)\Gamma(2-\alpha)\nu_v^\alpha\mathbf{E}_v^{n+1}}{\big(h^{1-\alpha} + \phi(h)\Gamma(2-\alpha)\mu_v^\alpha\big)},
\end{aligned} \tag{5.4}$$

and

$$\mathbf{N}^{n+1} = \frac{h^{1-\alpha}\mathbf{N}^n - \sum_{j=0}^{n-1} \Delta_{\alpha,n}^{j}(\mathbf{N}^{j+1} - \mathbf{N}^{j}) + \phi_\alpha(h)\Gamma(2-\alpha)\Lambda^\alpha}{\big(h^{1-\alpha} + \phi_\alpha(h)\Gamma(2-\alpha)\mu^\alpha\big)}. \tag{5.5}$$

Setting $n = 0$, the equation 5.5 gives

$$\mathbf{N}^1 = \frac{h^{1-\alpha}\mathbf{N}^0}{h^{1-\alpha} + \phi_\alpha(h)\Gamma(2-\alpha)\mu^\alpha} + \frac{\phi_\alpha(h)\Gamma(2-\alpha)\Lambda^\alpha}{h^{1-\alpha} + \phi_\alpha(h)\Gamma(2-\alpha)\mu^\alpha}. \tag{5.6}$$

The exact solution of the equation (5.2) is derived by using the Laplace transform technique introduced by Podlubny [**86**]

$$\mathbf{N}(t) = \mathbf{N}(0)E_\alpha\big(-(\mu t)^\alpha\big) + \Lambda^\alpha E_{\alpha,\alpha+1}\big(-(\mu t)^\alpha\big), \tag{5.7}$$

where $E_{\alpha,\alpha+1}$ is the Mittag-Leffler function

$$E_{\alpha,\beta}(t) = \sum_{k=0}^{\infty} \frac{t^k}{\Gamma(\alpha k + \beta)}, \quad (\alpha > 0,\ \beta > 0).$$

The denominator function $\phi_\alpha(h)$ can be derived by comparing the exact version (5.7) with the discrete version (5.6), that is

$$\phi_\alpha(h) = \frac{h^{1-\alpha}\Big(1 - E_\alpha\big(-(\mu h)^\alpha\big)\Big)}{E_\alpha\big(-(\mu h)^\alpha\big)\Gamma(2-\alpha)\mu^\alpha}.$$

It is not difficult to show that $\phi_\alpha(h)$ reduces to the classical $\phi(h)$ in (4.12) when $\alpha = 1$.

6. Numerical Results

In this section, we present the numerical solution of the systems (2.3) and (2.7) using the NSFD schema. Then, we compare it with the solution computed by the `ode45` solver of Matlab.

6.1. The human-mosquito Model. We denote by Y the matrix of order $N \times 7$ that contains the approximated solution determined by the `ode45` solver which is given by

$$Y = \begin{pmatrix} \mathbf{S}_h(t_1) & \mathbf{E}_h(t_1) & \mathbf{I}_h(t_1) & \mathbf{R}_h(t_1) & \mathbf{S}_v(t_1) & \mathbf{E}_v(t_1) & \mathbf{I}_v(t_1) \\ \mathbf{S}_h(t_2) & \mathbf{E}_h(t_2) & \mathbf{I}_h(t_2) & \mathbf{R}_h(t_2) & \mathbf{S}_v(t_2) & \mathbf{E}_v(t_2) & \mathbf{I}_v(t_2) \\ \vdots & \vdots & \vdots & \vdots & \vdots & \vdots & \vdots \\ \mathbf{S}_h(t_N) & \mathbf{E}_h(t_N) & \mathbf{I}_h(t_N) & \mathbf{R}_h(t_N) & \mathbf{S}_v(t_N) & \mathbf{E}_v(t_N) & \mathbf{I}_v(t_N) \end{pmatrix},$$

where N is the number of discretization points in time $t \in [0, T]$ and $t_i = (i-1) \times \frac{T}{N-1}$ for $i = 1, 2, \ldots, N$.

The parameters used to simulate the model are listed in the Table 1. The initial conditions are always set to

$$\mathbf{S}_h(0) = 0.9, \quad \mathbf{E}_h(0) = 0, \quad \mathbf{I}_h(0) = 0.1, \quad \mathbf{R}_h(0) = 0,$$
$$\mathbf{S}_v(0) = 0.88, \quad \mathbf{E}_v(0) = 0, \quad \mathbf{I}_v(0) = 0.12.$$

TABLE 1. Fixed and operational parameters for disease-free and disease-endemic equilibrium.

	E_0	E_1
μ_h	$3.8587e-04$	$3.8587e-04$
B	0.155	0.1932
β_{hv}	0.1254	0.773
β_{vh}	0.1149	0.7913
ν_h	0.0833	0.0833
η_h	0.2	0.2
μ_v	0.0333	0.0333
ν_v	0.1	0.1
N_h	$1e+6$	$1e+6$
N_v	$10 \times N_h$	$10 \times N_h$
T (days)	30×365	5×365

The following Figures 3–8 represent the three dimensional curves of the human and the vector populations, respectively. They show that the NSFD method remains stable and approaches the disease-free equilibrium (DFE) or endemic equilibrium (EE) points.

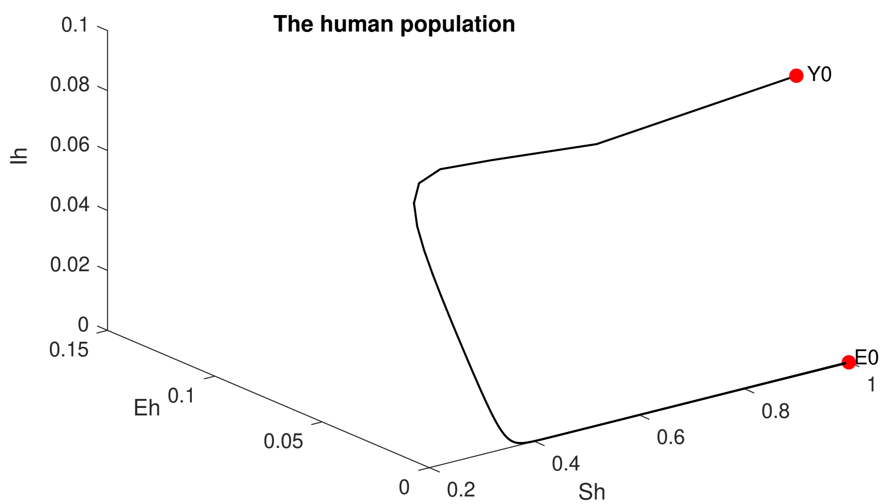

FIGURE 3. The convergence of the discrete system (4.3) to the DFE

The Figures 9 and 10 show that the approximate solutions obtained by the NSFD method and `ode45` method are very closed to each other. However, the solution Y obtained by the `ode45` solver becomes negative for some values of t. This does not figure clearly in the curves because the smallest negative value of Y is $-1.19e-6$.

The Table 2 presents the percentage of negative values in the matrix Y simulating the human-mosquito model (2.3) with the `ode45` solver using the parameters for the disease-free point in the Table 1. The results given in Table 2 show that the NSFD preserves the positivity for all step sizes in $[0, T]$ which is a desirable modeling property. On the other side, the `ode45` method yields solutions that becomes negative for some value of t.

6.2. The human-mosquito-monkey model. Now we simulate the system for the data given in Tables 2 and 2. The initial conditions are always set to

$$\mathbf{S}_m(0) = 0.8, \quad \mathbf{E}_m(0) = 0, \quad \mathbf{I}_m(0) = 0.8, \quad \mathbf{R}_m(0) = 0.$$

Figures 11–20 show that the numerical solution approximates very well the solution of the continuous system by preserving positivity and converging towards the equilibrium points DFE or EE. Table 4 gives the percentage of negative values for the NSFD method and the `ode45` solver. It can easily be seen that NSFD preserves the positivity of the continuous system where the `ode45` solver failed in some cases.

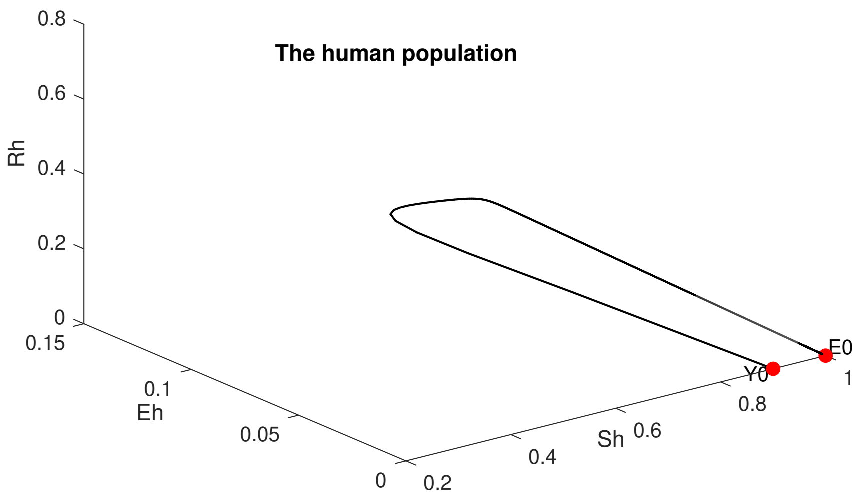

FIGURE 4. The convergence of the discrete system (4.3) to the DFE

TABLE 2. Percentage of negative paths for the NSFD method and the standard `ode45` solver .

	N=60	N=100	N=400	N=1200	N=2000	N=3000	N=5000
NSFD	0	0	0	0	0	0	0
ode45	26.67%	26.71%	27%	27.07%	27.05%	27.06%	27.07%
min(Y)	-1.14e-06	-1.09e-6	-1.1e-6	-1.19e-6	-1.14	-1.17e-6	-1.19e-6

6.3. The time-fractional model. In this section, we provide some numerical simulations of the discrete model (5.4) with different values of fractional order α. To proceed with the simulation, we use the parameter values in Table 1 and the initial conditions in (6.1). The numerical simulation results for the NSFD fractional order obtained for different values of α are displayed in Figures. 21-26. These figures show two different scenarios:

Case 1 DFE. : The dynamical behavior of system for different values of α is shown in Figures 21-23 for $R_0^\alpha < 1$ which implies that it converges to the DFE. It is noticeable that due to the memory property of the Caputo fractional derivatives, the evolution of the system becomes slower each time the α decreases. Therefore, the system decays to the equilibrium like $t^{-\alpha}$, as previously established in [**69**].

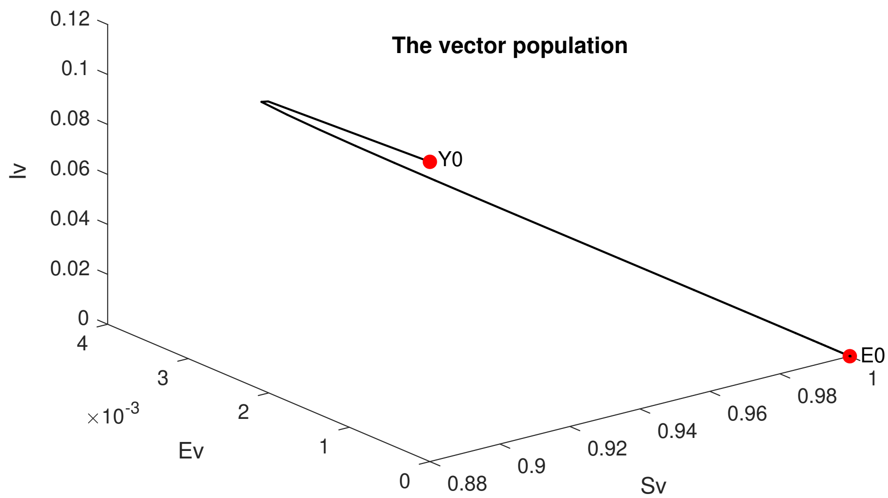

FIGURE 5. The convergence of the discrete system (4.3) to the DFE

TABLE 3. Fixed and operational parameters for disease-free and disease-endemic equilibria (Monkey population).

	E_0	E_1
μ_m	$3.87e-2$	$3.87e-2$
β_{mv}	0.1254	0.773
β_{vm}	0.1149	0.7913
ν_m	0.035	0.035
η_m	0.3	0.2
N_m	$3.3e5$	$3.3e5$
T (days)	365×30	365×2

Case 2 EE.: For $R_0^\alpha > 1$, Figures 24-26 show the impact of changing the Caputo fractional order α on Zika dynamics. The observed behavior from these figures demonstrates that the EE is shifted towards $E_{\alpha_1}, E_{\alpha_2}, E_{\alpha 3}$ and E_{α_4} when α is decreasing which confirms the validity of stability analysis represented in Appendix.

The numerical results above show the memory effect for the fractional dynamical system which does not occur in the ordinary differential system as already

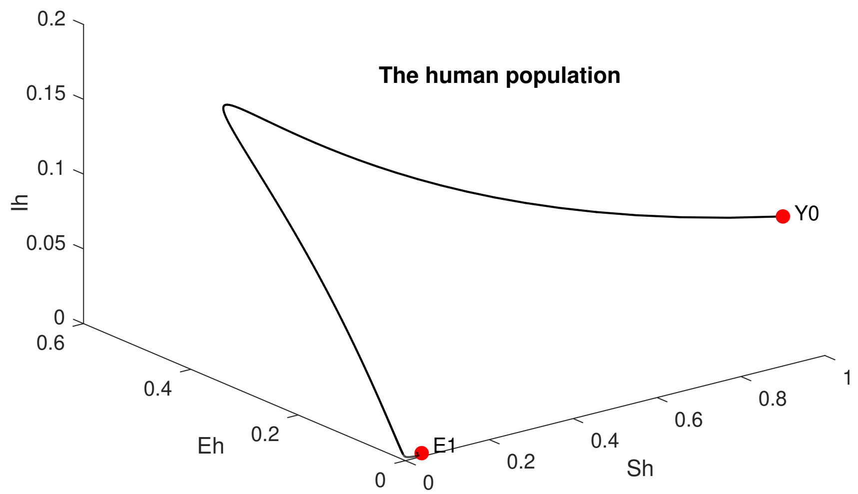

FIGURE 6. The convergence of the discrete system (4.3) to the EE

TABLE 4. Percentage of negative paths for the NSFD method and `ode45` solver.

	N=60	N=100	N=400	N=1200	N=2000	N=3000	N=5000
NSFD	0	0	0	0	0	0	0
ode45	27.73%	27.73%	28.43%	28.22%	28.42%	28.36%	28.4%
min(Y)	-1.02e-6	-1.12e-6	-1.12e-6	-1.2e-6	-1.12e-6	-1.18e-6	-1.18e-6

proved by [**7, 8**]. And show also that the new approach is very effective, preserves the positivity of the system, applies simpler and can be used as an alternate method for solving fractional differential problems.

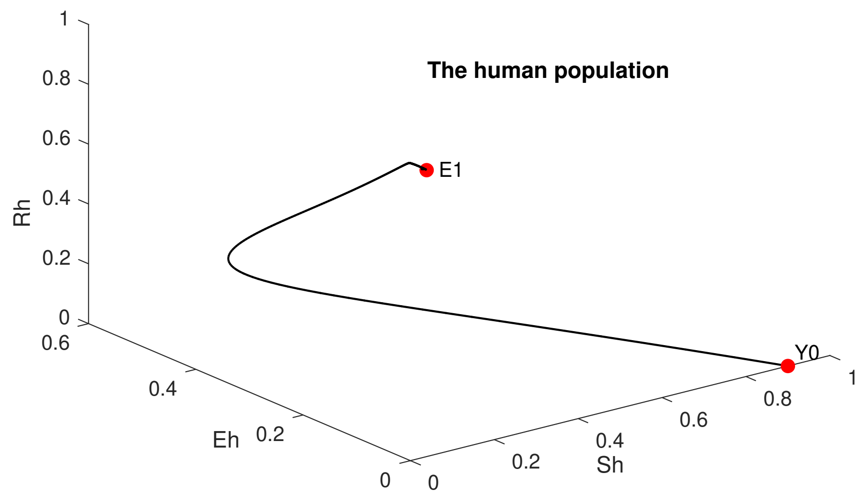

FIGURE 7. The convergence of the discrete system (4.3) to the EE

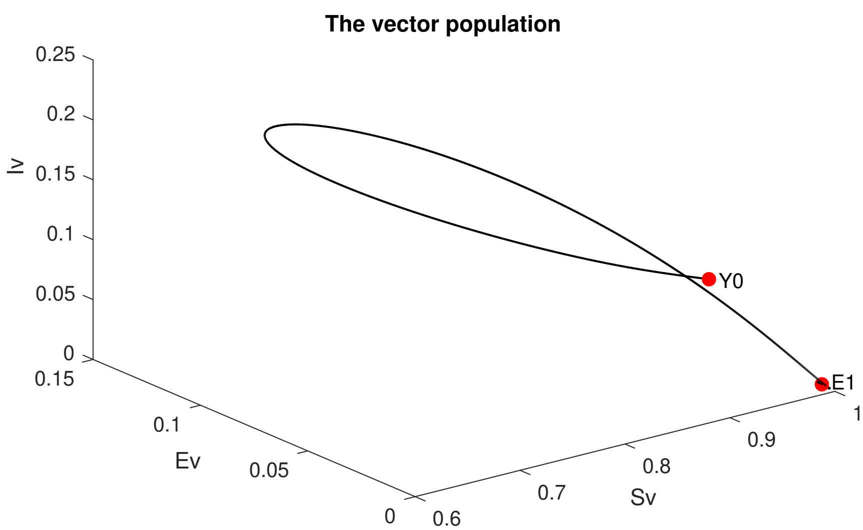

FIGURE 8. The convergence of the discrete system (4.3) to the EE

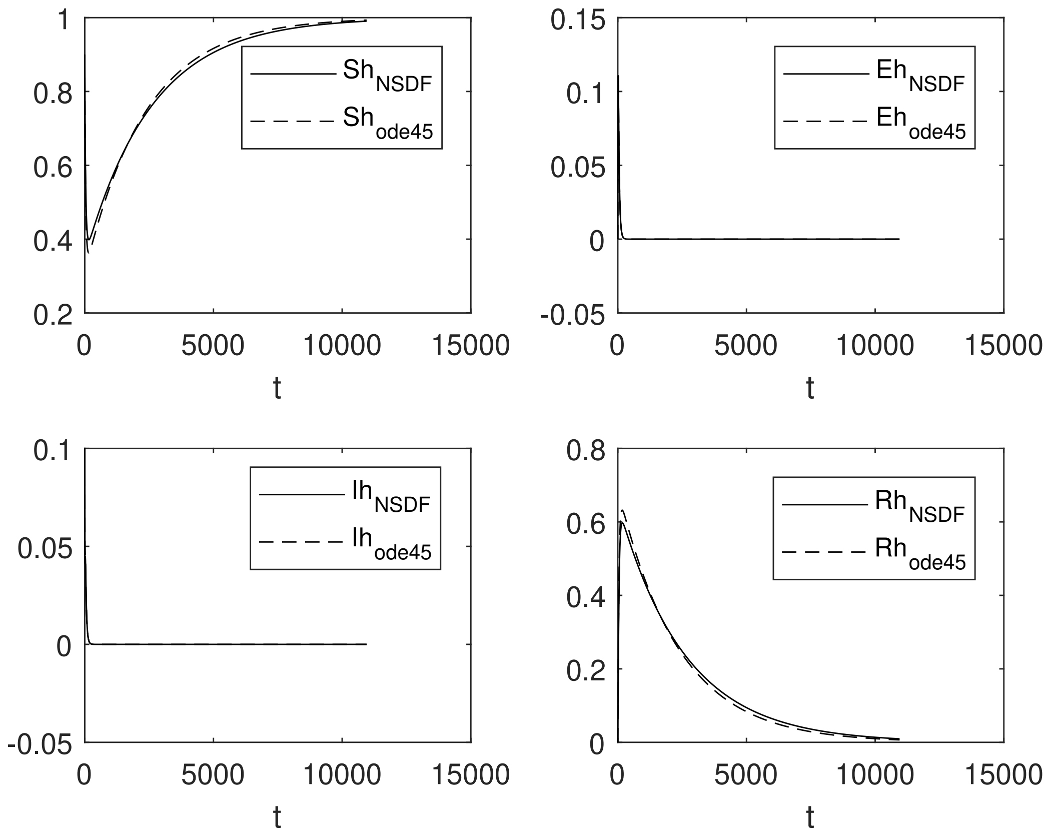

FIGURE 9. The NSFD and `ode45` method numerical simulations of human sub-populations $S_h(t)$, $E_h(t)$, $I_h(t)$ and $R_h(t)$ for model (2.3).

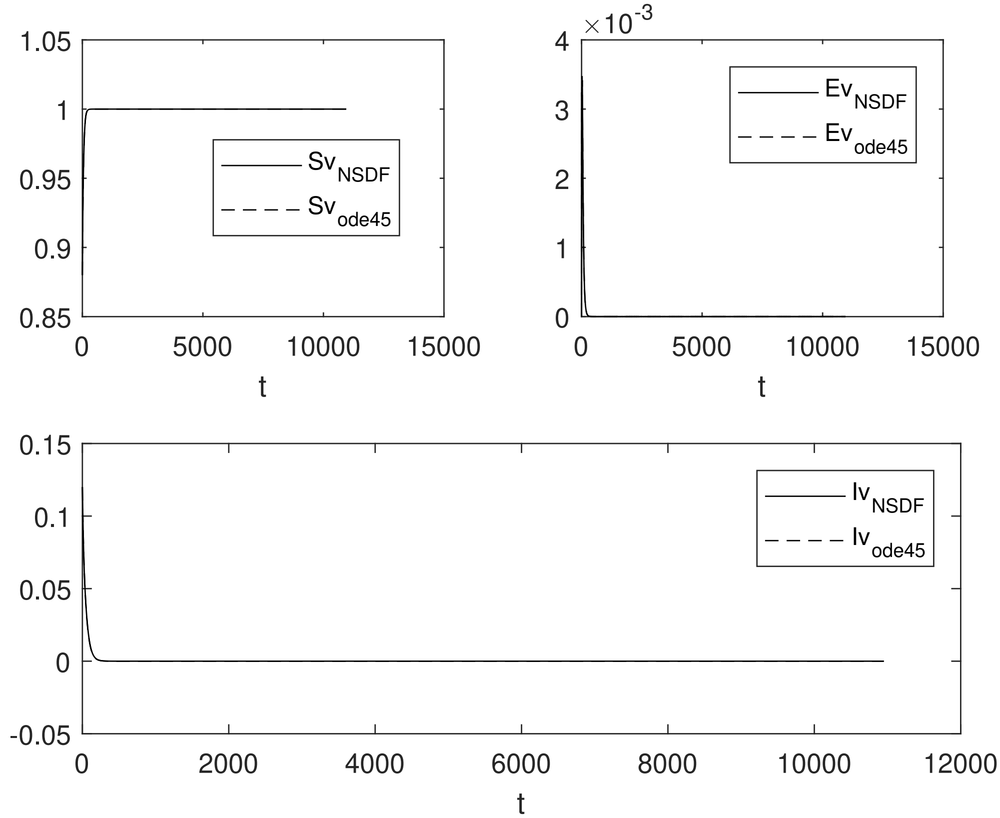

Figure 10. The NSFD and `ode45` method numerical simulations of vector sub-populations $S_v(t)$, $E_v(t)$ and $I_v(t)$ for model (2.3).

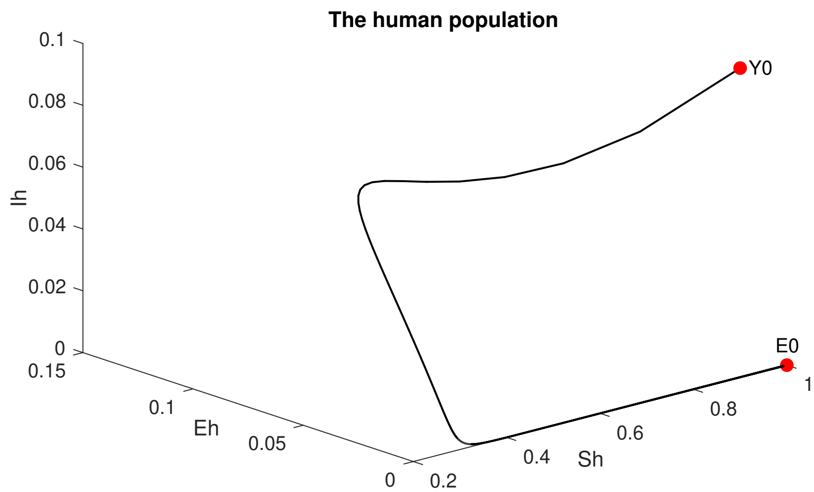

FIGURE 11. The convergence of the discrete system (4.5) to the DFE

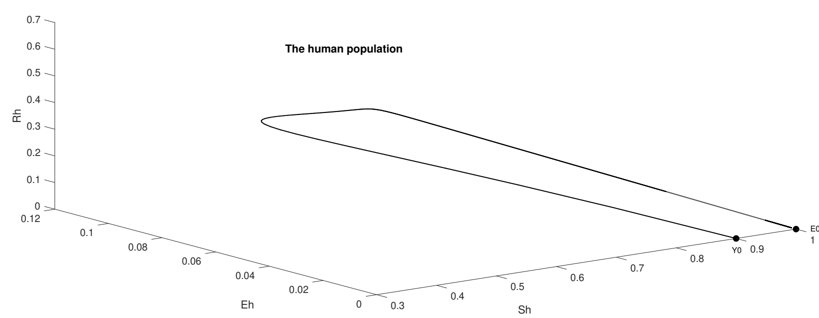

FIGURE 12. The convergence of the discrete system (4.5) to the DFE

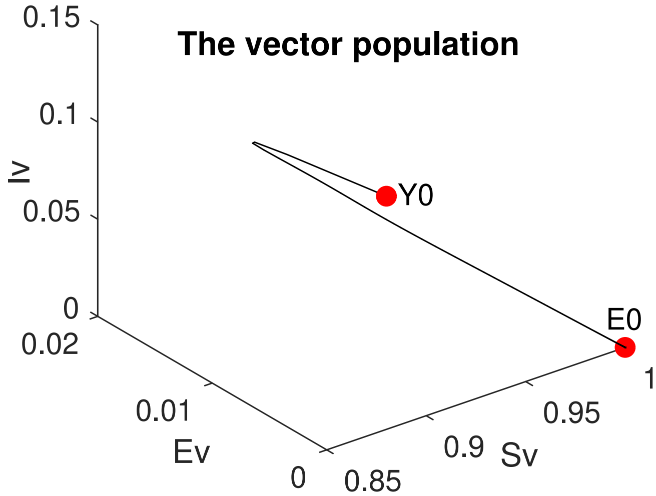

FIGURE 13. The convergence of the discrete system (4.5) to the DFE

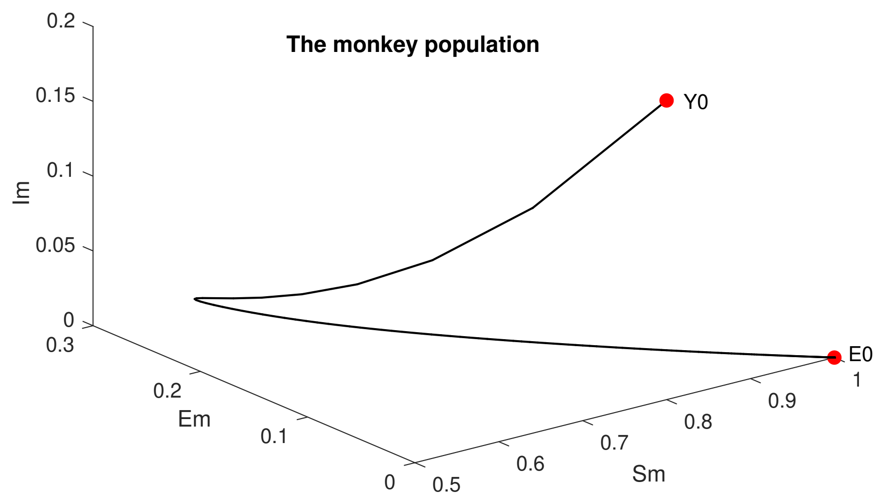

FIGURE 14. The convergence of the discrete system (4.5) to the DFE

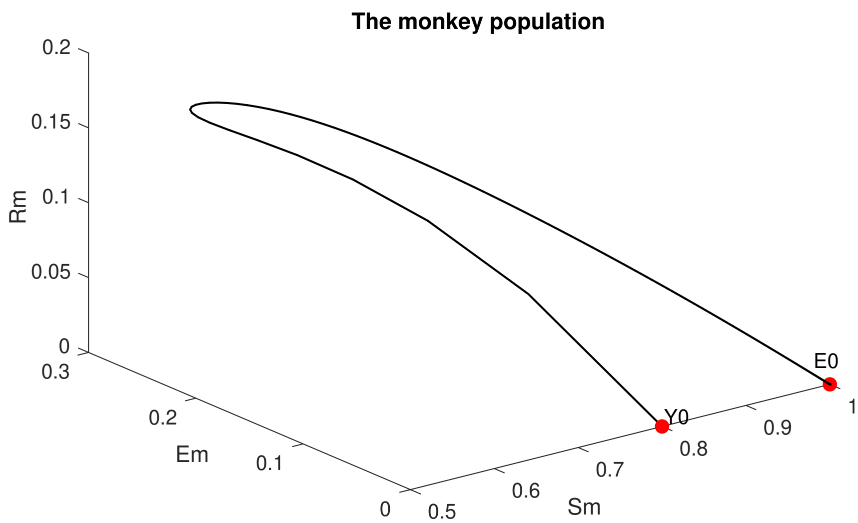

FIGURE 15. The convergence of the discrete system (4.5) to the DFE

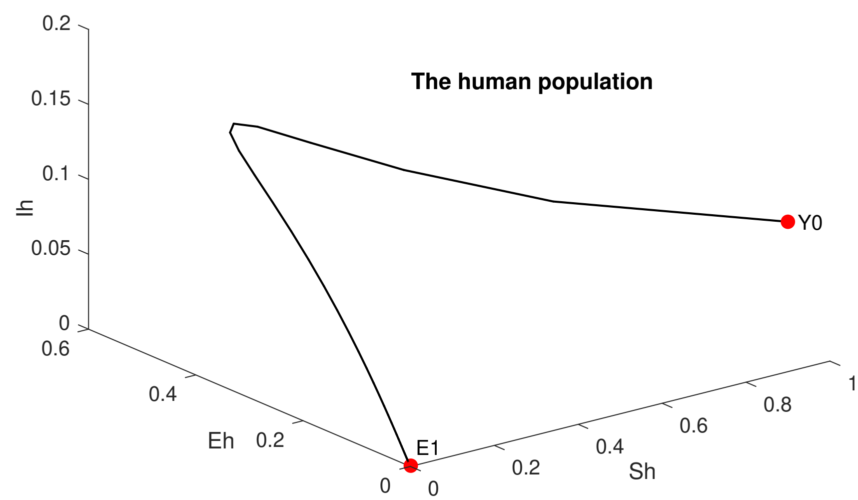

FIGURE 16. The convergence of the discrete system (4.5) to the EE

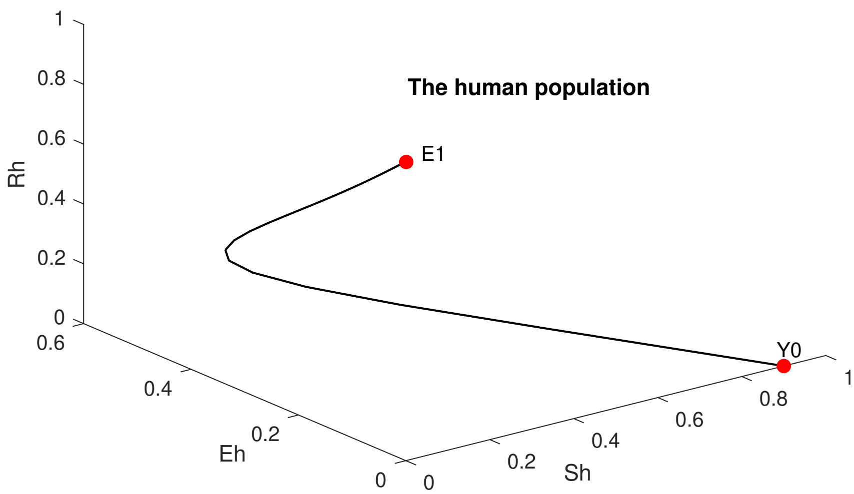

FIGURE 17. The convergence of the discrete system (4.5) to the EE

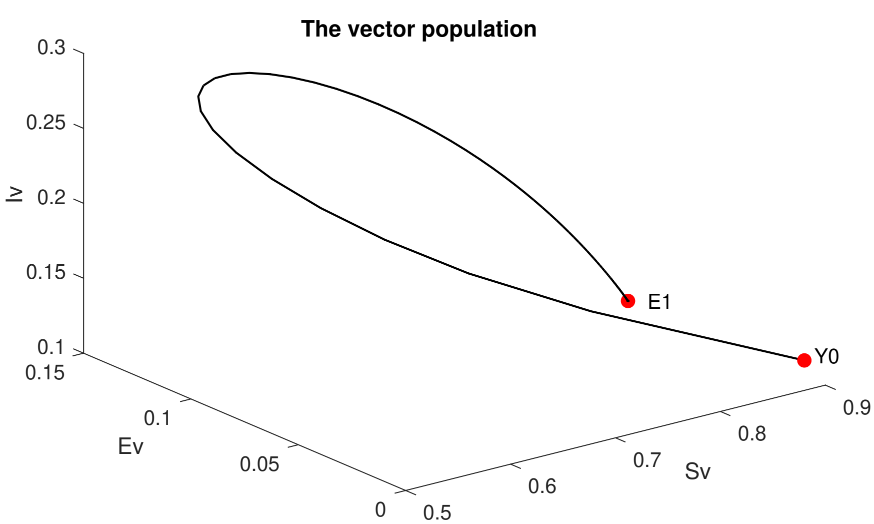

FIGURE 18. The convergence of the discrete system (4.5) to the EE

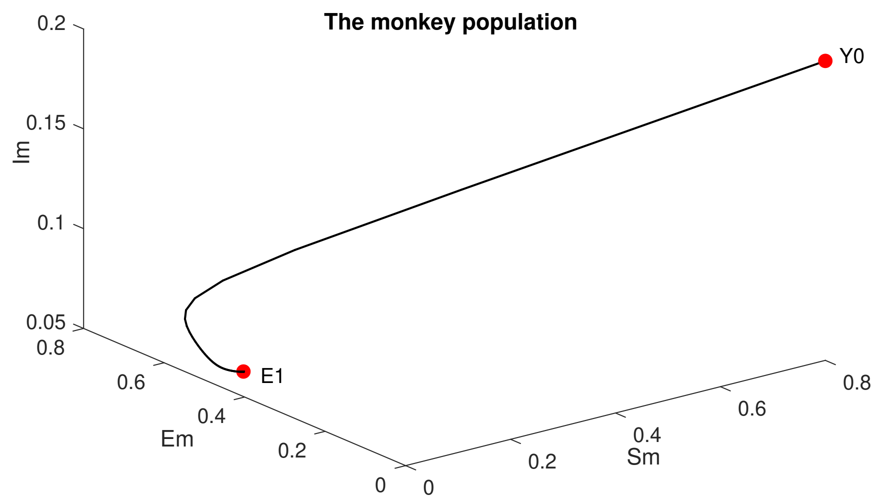

FIGURE 19. The convergence of the discrete system (4.5) to the EE

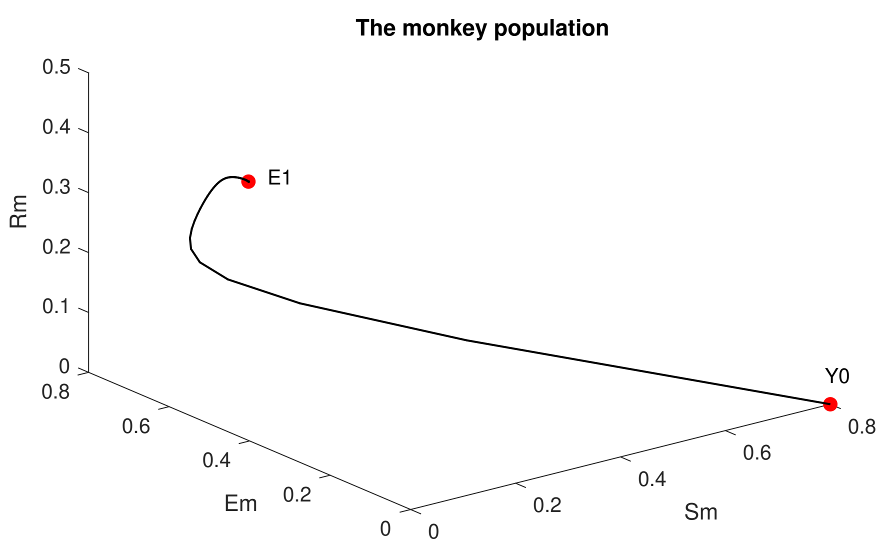

FIGURE 20. The convergence of the discrete system (4.5) to the EE

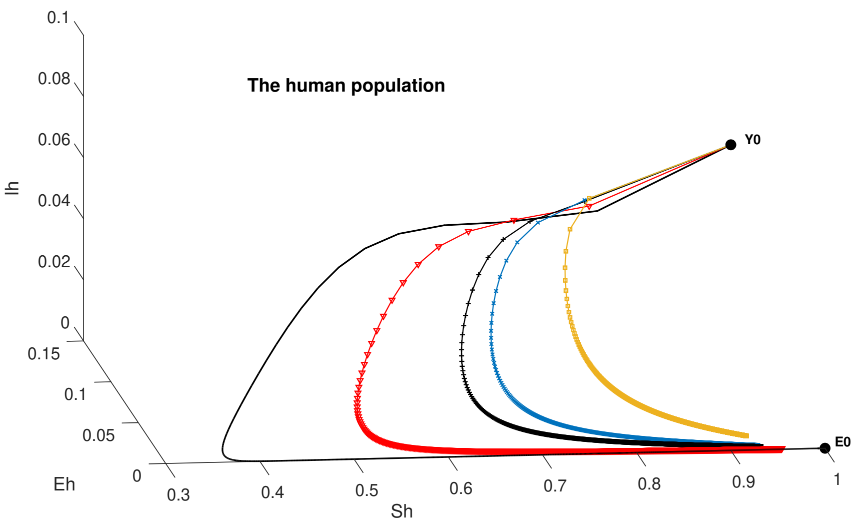

FIGURE 21. The convergence of the discrete fractional system (5.4) to the DFE.

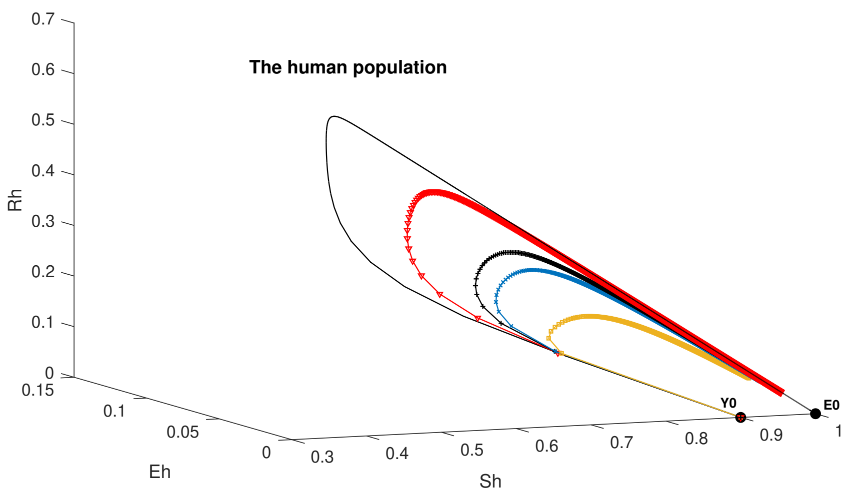

FIGURE 22. The convergence of the discrete fractional system (5.4) to the DFE.

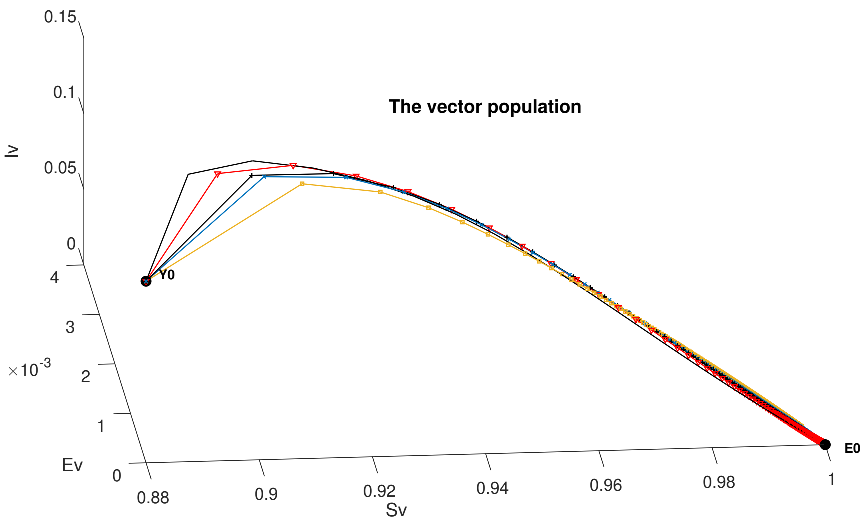

FIGURE 23. The convergence of the discrete fractional system (5.4) to the DFE.

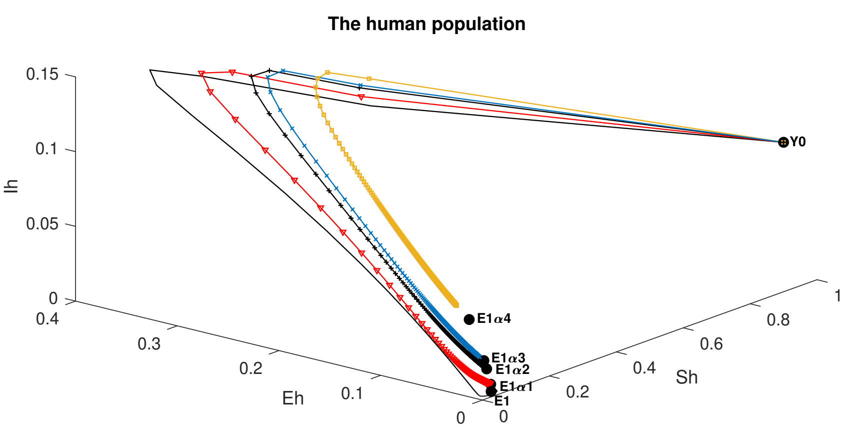

FIGURE 24. The convergence of the discrete fractional system (5.4) to the EE.

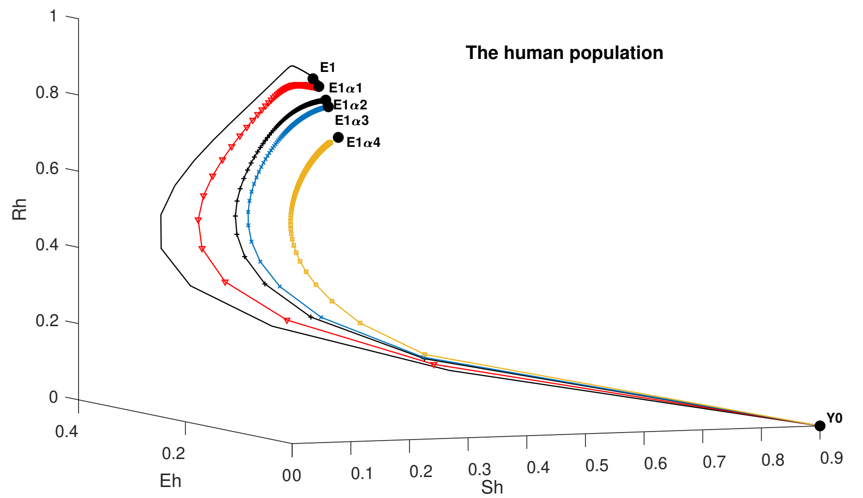

FIGURE 25. The convergence of the discrete fractional system (5.4) to the EE.

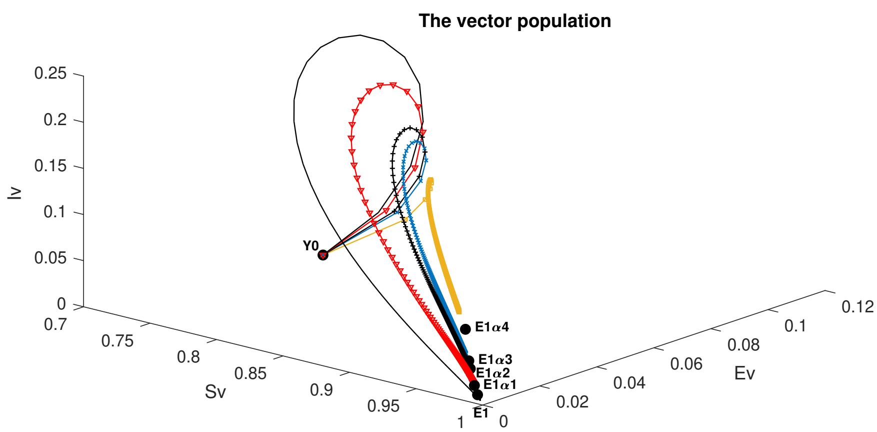

FIGURE 26. The convergence of the discrete fractional system (5.4) to the EE.

7. Conclusion and Outlook

In this work we have presented a novel nonstandard finite difference (NSFD) method for calculating numerical solutions to a SEIR model for the spread of the Zika virus. In the absence of the exact solution and in order to prove the efficiency of the method, the approximate solution is compared with the `ode45` solver solution. The numerical simulations show that the discrete system converges to the same equilibrium points as that of the continuous system. They also prove that the positivity is preserved. Finally, it should be clear that the use of the NSFD methodology can be applied to all epidemic models of the spread of diseases.

It is worth recalling that we have used Caputo-type fractional derivatives to describe the temporal dynamics of epidemiological models. The most important reason for using a system of ODEs/PDEs of time-fractional order equations is to account for memory effects. These types of effects exist e.g. in many realistic systems like in endemic models to describe the waning effects of the vaccination or a biphasic decline behavior of infections or diseases.

These fractional order approaches were used in COVID-19 transmission models by using fractional order Caputo derivative [**90**], the analysis of semi-analytical solutions of a hepatitis B epidemic model using the Caputo-Fabrizio operator [**5**], the study of stability and Lyapunov functions for HIV/AIDS epidemic models with the Atangana-Baleanu-Caputo derivative [**97**], the mathematical modeling of the measles epidemic with optimized fractional order under the classical Caputo differential operator [**88**].

Appendix

7.1. The human-mosquito-monkey model. The system (2.7) has two equilibrium points, the disease-free equilibrium $E_0 = (1,0,0,0,1,0,0,1,0,0,0)^\top$ and the endemic equilibrium $E_1^{**} = (\mathbf{S}_h^{**}, \mathbf{E}_h^{**}, \mathbf{I}_h^{**}, \mathbf{S}_v^{**}, \mathbf{I}_v^{**}, \mathbf{S}_m^{**}, \mathbf{E}_m^{**}, \mathbf{I}_m^{**})^\top$, where

$$\begin{aligned}
\mathbf{S}_h^{**} &= \frac{\mu_h N_h}{B\beta_{vh} N_v \mathbf{I}_v + \mu_h N_h},\\
\mathbf{E}_h^{**} &= \frac{\mu_h B\beta_{vh} N_v \mathbf{I}_v^{**}}{(\nu_h+\mu_h)(B\beta_{vh} N_v \mathbf{I}_v^{**} + \mu_h N_h)},\\
\mathbf{I}_h^{**} &= \frac{\nu_h \mathbf{E}_h^{**}}{(\eta_h+\mu_h)},\\
\mathbf{S}_v^{**} &= \frac{\nu_v - (\nu_v+\mu_v)\mathbf{I}_v^{**}}{\nu_v},\\
\mathbf{S}_m^{**} &= \frac{\mu_m N_m}{B\beta_{vm} N_v \mathbf{I}_v^{**} + \mu_m N_m},\\
\mathbf{E}_m^{**} &= \frac{\mu_m B\beta_{vm} N_v \mathbf{I}_v^{**}}{(\nu_m+\mu_m)(B\beta_{vm} N_v \mathbf{I}_v^{**} + \mu_m N_m)},\\
\mathbf{I}_m^{**} &= \frac{\nu_m}{(\eta_m+\mu_m)}\mathbf{E}_m^{**},
\end{aligned} \tag{7.1}$$

$\mathbf{I}_v^{**}$ is implicitly given as the zero of the following rational fraction expression

$$P(\mathbf{I}_v) = \frac{\nu_h \mu_h B\beta_{hv} B\beta_{vh} N_v \big(\nu_v - (\nu_v+\mu_v)\mathbf{I}_v\big)}{(\eta_h+\mu_h)(\nu_h+\mu_h)(B\beta_{vh} N_v \mathbf{I}_v + \mu_h N_h)}$$

$$+\frac{\nu_m\mu_m B\beta_{mv}B\beta_{vm}N_v\big(\nu_v-(\nu_v+\mu_v)\mathbf{I}_v\big)}{(\eta_m+\mu_m)(\nu_m+\mu_m)(B\beta_{vm}N_v\mathbf{I}_v+\mu_m N_m)}-\mu_v(\nu_v+\mu_v),$$

which is determined numerically. The basic reproduction number of (2.7) is

$$R_0=\sqrt{R_{0,1}+R_{0,2}},$$

where

$$R_{0,1}=\frac{\nu_v\nu_m B\beta_{vm}B\beta_{mv}N_v}{\mu_v(\mu_v+\nu_v)(\mu_m+\nu_m)(\mu_m+\eta_m)N_m},$$

and

$$R_{0,2}=\frac{B\nu_v\nu_h B\beta_{vh}\beta_{hv}N_v}{\mu_v(\mu_v+\nu_v)(\mu_h+\nu_h)(\mu_h+\eta_h)N_h}.$$

7.2. The time-fractional model. The basic reproduction number R_0^α of the system (5.1) is given by

$$R_0^\alpha=\sqrt{\frac{\nu_h^\alpha\nu_v^\alpha B^\alpha\beta_{vh}B^\alpha\beta_{hv}N_v}{\mu_v^\alpha(\nu_h^\alpha+\mu_h^\alpha)(\eta_h^\alpha+\mu_h^\alpha)(\mu_v^\alpha+\nu_v^\alpha)N_h}}.$$

THEOREM 7.1 (Equilibrium points, [**64**]). *Let us consider the definition domain*

$$\Omega=\big\{(\mathbf{S}_h,\mathbf{E}_h,\mathbf{I}_h,\mathbf{E}_v,\mathbf{I}_v)\in\mathbb{R}_+^5: 0\ \le \mathbf{S}_h+\mathbf{E}_h+\mathbf{I}_h\le 1;\ 0\le \mathbf{S}_v+\mathbf{I}_v\le 1\big\}.$$

The system (5.1) *has the disease-free equilibrium* $E_0=(1,0,0,1,0)$ *independent of the values of the parameters, whereas, only if* $R_0^\alpha>1$ *there exist a unique endemic equilibrium* $E_1=(\mathbf{S}_h^{**},\mathbf{E}_h^{**},\mathbf{I}_h^{**},\mathbf{S}_v^{**},\mathbf{I}_v^{**})$ *with*

$$\mathbf{S}_h^{**}=\frac{\mu_h^\alpha N_h}{B^\alpha\beta_{vh}N_v\mathbf{I}_v^{**}+\mu_h^\alpha N_h},\quad \mathbf{E}_h^{**}=\frac{(\eta_h^\alpha+\mu_h^\alpha)}{\nu_h^\alpha}\mathbf{I}_h^{**},$$
$$\mathbf{S}_v^{**}=\frac{\mu_v^\alpha}{(B^\alpha\beta_{hv}\mathbf{I}_h^{**}+\mu_v^\alpha)},\quad \mathbf{I}_v^{**}=\frac{\nu_v^\alpha}{(\mu_v^\alpha+\nu_v^\alpha)}\frac{B^\alpha\beta_{hv}\mathbf{I}_h^{**}}{(B^\alpha\beta_{hv}\mathbf{I}_h+\mu_v^\alpha)},$$

in the interior of Ω *where*

$$\mathbf{I}_h^{**}=\frac{\mu_v^\alpha\mu_h^\alpha(\mu_v^\alpha+\nu_v^\alpha)\big((R_0^\alpha)^2-1\big)}{B^\alpha\beta_{hv}\big(\nu_v^\alpha B^\alpha\beta_{vh}p+\mu_h^\alpha(\mu_v^\alpha+\nu_v^\alpha)\big)}.$$

The proof of the theorem requires the following lemma :

LEMMA 7.2. *If* $X^0,X^1,\dots,X^n\ge 0$ *then*

$$h^{1-\alpha}X^n-\sum_{j=0}^{n-1}\Delta_{\alpha,n}^j\big(X^{j+1}-X^j\big)\ge 0.$$

PROOF. For $n\in\mathbb{N}^*$, we have

$$h^{1-\alpha}X^n-\sum_{j=0}^{n-1}\Delta_{\alpha,n}^j\big(X^{j+1}-X^j\big)=\big(h^{1-\alpha}-\Delta_{\alpha,n}^{n-1}\big)X^n+\Delta_{\alpha,n}^0X^0+\sum_{j=1}^{n-1}\big(\Delta_{\alpha,n}^j-\Delta_{\alpha,n}^{j-1}\big)X^j.$$

and

$$h^{1-\alpha}-\Delta_{\alpha,n}^{n-1}=\big(2-2^{1-\alpha}\big)h^{1-\alpha}\ge 0.$$

Thus

$$h^{1-\alpha}X^n-\sum_{j=0}^{n-1}\Delta_{\alpha,n}^j\big(X^{j+1}-X^j\big)\ge 0$$

□

THEOREM 7.3 (Positivity of solution). *Let the initial data* $\mathbf{S}_h^0$, $\mathbf{E}_h^0$, $\mathbf{I}_h^0$, $\mathbf{R}_h^0$, $\mathbf{S}_v^0$, $\mathbf{E}_v^0$ *and* $\mathbf{I}_v^0 \geq 0$, *then all the components* $\mathbf{S}_h^{n+1}$, $\mathbf{E}_h^{n+1}$, $\mathbf{I}_h^{n+1}$, $\mathbf{R}_h^{n+1}$, $\mathbf{S}_v^{n+1}$, $\mathbf{E}_v^{n+1}$ *and* $\mathbf{I}_v^{n+1} \geq 0$ *in the system* (5.4) *are satisfied for all* $n \in \mathbb{N}$.

PROOF. We have for $n = 0$

$$\begin{aligned}
\mathbf{S}_h^1 &= \frac{h^{1-\alpha}\mathbf{S}_h^0 + \Gamma(2-\alpha)\phi_\alpha(h)\mu_h^\alpha}{\left(h^{1-\alpha} + \Gamma(2-\alpha)\phi_\alpha(h)\left(B^\alpha\beta_{vh}\dfrac{N_v}{N_h}\mathbf{I}_v^0 + \mu_h^\alpha\right)\right)} \geq 0,\\
\mathbf{E}_h^1 &= \frac{h^{1-\alpha}\mathbf{E}_h^0 + \Gamma(2-\alpha)\phi_\alpha(h)B^\alpha\beta_{vh}\dfrac{N_v}{N_h}\mathbf{I}_v^0\mathbf{S}_h^1}{\left(h^{1-\alpha} + \Gamma(2-\alpha)\phi_\alpha(h)(\nu_h^\alpha + \mu_h^\alpha)\right)} \geq 0,\\
\mathbf{I}_h^1 &= \frac{h^{1-\alpha}\mathbf{I}_h^0 + \Gamma(2-\alpha)\phi_\alpha(h)\nu_h^\alpha\mathbf{E}_h^1}{\left(h^{1-\alpha} + \Gamma(2-\alpha)\phi_\alpha(h)(\eta_h^\alpha + \mu_h^\alpha)\right)} \geq 0,\\
\mathbf{R}_h^1 &= \frac{h^{1-\alpha}\mathbf{R}_h^0 + \phi_\alpha(h)\Gamma(2-\alpha)\eta_h^\alpha\mathbf{I}_h^1}{\left(h^{1-\alpha} + \phi_\alpha(h)\Gamma(2-\alpha)\mu_h^\alpha\right)} \geq 0,\\
\mathbf{S}_v^1 &= \frac{h^{1-\alpha}\mathbf{S}_v^0 + \phi_\alpha(h)\Gamma(2-\alpha)\mu_v^\alpha}{\left(h^{1-\alpha} + \phi_\alpha(h)\Gamma(2-\alpha)(B^\alpha\beta_{hv}\mathbf{I}_h^1 + \mu_v^\alpha)\right)} \geq 0,\\
\mathbf{E}_v^1 &= \frac{h^{1-\alpha}\mathbf{E}_v^0 + \phi_\alpha(h)\Gamma(2-\alpha)B^\alpha\beta_{hv}\mathbf{I}_h^1\mathbf{S}_v^1}{\left(h^{1-\alpha} + \phi_\alpha(h)\Gamma(2-\alpha)(\nu_v^\alpha + \mu_v^\alpha)\right)} \geq 0,\\
\mathbf{I}_v^1 &= \frac{h^{1-\alpha}\mathbf{I}_v^0 + \phi_\alpha(h)\Gamma(2-\alpha)\nu_v^\alpha\mathbf{E}_v^1}{\left(h^{1-\alpha} + \phi_\alpha(h)\Gamma(2-\alpha)\mu_v^\alpha\right)} \geq 0.
\end{aligned}$$

We suppose that for $1, 2, \ldots, n$, $\mathbf{S}_h^n$, $\mathbf{E}_h^n$, $\mathbf{I}_h^n$, $\mathbf{R}_h^n$, $\mathbf{S}_v^n$, $\mathbf{E}_v^n$ and $\mathbf{I}_v^n \geq 0$. The hypothesis of induction and Lemma 7.2 allow for $n+1$, i.e.

$$\mathbf{S}_h^{n+1},\ \mathbf{E}_h^{n+1},\ \mathbf{I}_h^{n+1},\ \mathbf{R}_h^{n+1},\ \mathbf{S}_v^{n+1},\ \mathbf{E}_v^{n+1}\ \text{ and }\ \mathbf{I}_v^{n+1} \geq 0.$$

□

References

[1] M.A. Aba Oud, A. Ali, H. Alrabaiah, S. Ullah, M.A. Khan, and S. Islam, *A fractional order mathematical model for COVID-19 dynamics with quarantine, isolation, and environmental viral load*, Adv. Diff. Eqs. **2021(1)** (2021), 1–19.

[2] E. Addai, L. Zhang, J. Ackora-Prah, J.F. Gordon, J.K.K. Asamoah, and J.F. Essel, *Fractal-fractional order dynamics and numerical simulations of a Zika epidemic model with insecticide-treated nets*, Physica A: Stat. Mech. Appl. **603** (2022), 127809.

[3] F.B. Agusto, S. Bewick, and W.F. Fagan, *Mathematical model of Zika virus with vertical transmission*, Infect. Dis. Model. **2(2)** (2017), 244–267.

[4] F.B. Agusto, S. Bewick, and W.F. Fagan, *Mathematical model for Zika virus dynamics with sexual transmission route*, Ecolog. Compl. **29** (2017), 61–81.

[5] S. Ahmad, M. ur Rahman, and M. Arfan, *On the analysis of semi-analytical solutions of Hepatitis B epidemic model under the Caputo-Fabrizio operator*, Chaos, Solitons & Fractals **146** (2021), 110892.

[6] A. Ali, Q. Iqbal, J.K.K. Asamoah, and S. Islam, *Mathematical modeling for the transmission potential of Zika virus with optimal control strategies*, Europ. Phys. J. Plus, **137(1)** (2022), 1–30.

[7] A. Ali, S. Islam, M.R. Khan, S. Rasheed, F.M. Allehiany, J. Baili, M.A. Khan, and H. Ahmad, *Dynamics of a fractional order Zika virus model with mutant*, Alexandria Engrg. J. **61(6)** (2022), 4821–4836.

[8] A. Ali, F.S. Alshammari, S. Islam, M.A. Khan, and S. Ullah, *Modeling and analysis of the dynamics of novel coronavirus (COVID-19) with Caputo fractional derivative*, Results in Physics **20** (2021), 103669.

[9] H.M. Ali and I.G. Ameen, *Optimal control strategies of a fractional order model for Zika virus infection involving various transmissions*, Chaos, Solitons & Fractals **146** (2021), 110864.

[10] E.O. Alzahrani, W. Ahmad, M.A. Khan, and S.J. Malebary, *Optimal control strategies of Zika virus model with mutant*, Commun. Nonlin. Sci. Numer. Simul. 93 (2021), 105532.

[11] D.F. Aranda L., G. Gonzalez-Parra, and T. Benincasa, *Mathematical modeling and numerical simulations of Zika in Colombia considering mutation*, Math. Comput. Simul. **163** (2019), 1–18.

[12] A.Q.C. Araujo, M.T.T. Silva, and A.P.Q.C. Araujo, *Zika virus-associated neurological disorders: a review*, Brain **139** (2016), 2122–2130.

[13] L. Barbi, A.V.C. Coelho, L.C.A. Alencar, and S. Crovella, *Prevalence of Guillain-Barré syndrome among Zika virus infected cases: a systematic review and meta-analysis*, Brazil. J. Infect. Dis. **22** (2018), 137–141.

[14] R. Becker, *Animal models to study whether Zika causes birth defects*, Nat. Med. **22(3)** (2016), 225–227.

[15] R. Begum, O. Tunç, H. Khan, H. Gulzar, and A. Khan, *A fractional order Zika virus model with Mittag-Leffler kernel*, Chaos, Solitons & Fractals **146** (2021), 110898.

[16] S. Berkhahn and M. Ehrhardt, *A Physics-Informed Neural Network to Model COVID-19 Infection and Hospitalization Scenarios*, Adv. Cont. Discr. Mod. Theo. Appl. 2022, 61 (2022).

[17] K. Best and A.S. Perelson, *Mathematical modeling of within-host Zika virus dynamics*, Immunol. Rev. **285(1)** (2018), 81–96.

[18] S.K. Biswas, U. Ghosh, and S. Sarkar, *Mathematical model of Zika virus dynamics with vector control and sensitivity analysis*, Infect. Dis. Model. **5** (2020), 23–41.

[19] E. Bonyah and K.O. Okosun, *Mathematical modeling of Zika virus*, Asian Pac. J. Trop. Dis. **6(9)** (2016), 673–679.

[20] E. Bonyah, M.A. Khan, K.O. Okosun, and J.F. Gómez-Aguilar, *On the co-infection of dengue fever and Zika virus*, Optim. Contr. Appl. Meth. **40(3)** (2019), 394–421.

[21] E. Bonyah, M.A. Khan, K.O. Okosun, and S. Islam, *A theoretical model for Zika virus transmission*, PloS one, **12(10)** (2017), e0185540.

[22] J.P.T. Boorman and J.S. Porterfield, *A simple technique for infection of mosquitoes with viruses, transmission of Zika virus*, Trans. Roy. Soc. Trop. Med. Hyg. **50(3)** (1956), 238–242.

[23] L. Bouzid and O. Belhamiti, *Effect of seasonal changes on predictive model of bovine babesiosis transmission*, Int. J. Model. Simul. Sci. Comput. **8(4)** (2017), 1–17.

[24] F. Brauer and C. Castillo-Chávez, *Basic Ideas of Mathematical Epidemiology*, Mathematical Models in Population Biology and Epidemiology, Springer, 2001, pp. 275–337.

[25] Y. Cai, K. Wang, and W. Wang, *Global transmission dynamics of a Zika virus model*, Appl. Math. Lett. **92** (2019), 190–195.

[26] C.J. Carlson, E.R. Dougherty, and W. Getz, *An ecological assessment of the pandemic threat of Zika virus*, PLoS Neglected Trop. Dis. **10(8)** (2016), e0004968.

[27] C. Castillo-Chávez and R.H. Thieme, *Asymptotically autonomous epidemic models*, in: Mathematical Population Dynamics: Analysis of Heterogeneity, 0. Arimo, D.E. Axelrod, and M. Kimmel (eds.), Wuerz Publishing, Winnipeg, MB, Canada, 1995, pp. 33–50.

[28] S. Cauchemez, M. Besnard, P. Bompard, et al., *Association between Zika virus and microcephaly in French Polynesia, 2013-15: a retrospective study*, Lancet **387(10033)** (2016), 2125–2132.

[29] Y.-M. Chu, A. Aatif, M.A. Khan, S. Islam, and S. Ullah, *Dynamics of fractional order COVID-19 model with a case study of Saudi Arabia*, Results in Physics **21** (2021), 103787.

[30] F.R. Cugola, I.R. Fernandes, F.B. Russo, B.C Freitas, J.L.M. Dias, K.P. Guimarães, et al., *The Brazilian Zika virus strain causes birth defects in experimental models*, Nature 534 (2016), 267–271.

[31] M. Darwish, *A seroepidemiological survey for bunyaviridae and certain other arboviruses in Pakistan*, Trans. R. Soc. Trop. Med. Hyg. **77(4)** (1983), 446–450.

[32] G.W. Dick, S.F. Kitchen, and A.J. Haddow, *Zika virus. I. isolations and serological specificity*, Trans. R. Soc. Trop. Med. Hyg. **46(5)** (1952), 509–520.

[33] G.W. Dick, *Zika virus. II. pathogenicity and physical properties*, Trans. R. Soc. Trop. Med. Hyg. **46(5)** (1952), 521–534.

[34] L. Dinh, G. Chowell, K. Mizumoto, and H. Nishiura, *Estimating the subcritical transmissibility of the Zika outbreak in the state of Florida, USA, 2016*, Theoret. Biol. Med. Modell. **13(1)** (2016) 1–7.

[35] K. Diethelm, *A fractional calculus based model for the simulation of an outbreak of Dengue fever*, Nonlinear Dyn. **71** (2013), 613–619.

[36] M.R. Duffy, *Zika virus outbreak on Yap Island, federated states of Micronesia*, N. Engl. J. Med. **360(24)** (2009), 2536–2543.

[37] M. Ehrhardt and R.E. Mickens, *A Nonstandard Finite Difference Scheme for Solving a Zika Virus Model*, unpublished manuscript, 2017.

[38] M. Farman, A. Akgül, S. Askar, T. Botmart, A. Ahmad, and H. Ahmad, *Modeling and analysis of fractional order Zika model*, Virus **3** (2021), 4.

[39] A.S. Fauci and D.M. Morens, *Zika virus in the Americas - yet another arbovirus threat*, New England Journal of Medicine 374 (2016), 601–604.

[40] D. Gao, *Prevention and control of Zika as a mosquito-borne and sexually transmitted disease: a mathematical modeling analysis*, Sci. Rep. **6(28070)** (2016), 1–10.

[41] D. Gatherer and A. Kohl, *Zika virus: a previously slow pandemic spreads rapidly through the Americas*, J. Gen. Virol. **97(2)** (2016), 269–273.

[42] A. Gerisch and R. Weiner, *The positivity of low-order explicit Runge-Kutta schemes applied in splitting methods*, Comput. Math. Appl. **45** (2003), 53–67.

[43] C. Gokila and M. Sambath, *Modeling and simulations of a Zika virus as a mosquito-borne transmitted disease with environmental fluctuations*, Int. J. Nonl. Sci. Numer. Simul. (2021).

[44] B. Hasan, M. Singh, D. Richards, and A. Blicblau, *Mathematical modelling of Zika virus as a mosquito-borne and sexually transmitted disease with diffusion effects*, Math. Comput. Simulat. **166** (2019), 56–75.

[45] E.B. Hayes, *Zika virus outside Africa*, Emerg. Infect. Dis. **15(9)** (2009), 1347–1350.

[46] J.L. Helmersson, H. Stenlund, A.W. Smith, and J. Rocklö, *Vectorial capacity of Aedes Aegypti: effects of temperature and implications for global Dengue epidemic potential*, PLoS one **9(3)** (2014), 1–10.

[47] H.W. Hethcote, *The mathematics of infectious diseases*, SIAM Review **42** (2000), 599–653.

[48] S. Ioos, H.P. Mallet, I.L. Goffart, V. Gauthier, T. Cardoso, and M. Herida, *Current Zika virus epidemiology and recent epidemics*, Medecine et maladies infectieuses **44(7)** (2014), 302–307.

[49] R. Isea and K.E. Lonngren, *A preliminary mathematical model for the dynamic transmission of Dengue, Chikungunya and Zika*, Amer. J. Mod. Phys. Appl. **3(2)** (2016), 11–15.

[50] M. Jagan, M.S. deJonge, O. Krylova, and D.J.D. Earn, *Fast estimation of time-varying infectious disease transmission rates*, PLoS Comput. Biol. 16(9) (2020), e1008124.

[51] B. Jin, *Fractional differential equations*, Springer International Publishing, 2021.

[52] V.L.P. Junior, K. Luz, R. Parreira, and P. Ferrinho, *Zika virus: a review to clinicians*, Acta Médica Portuguesa **28(6)** (2015), 760–765.

[53] E.B. Kauffman, and L.D. Kramer, *Zika Virus Mosquito Vectors: Competence, Biology, and Vector Control*, J. Infect. Dis. **216** (2017), S976–S990.

[54] W.O. Kermack and A.G. McKendrick, *A contribution to the mathematical theory of epidemics*, Proc. R. Soc. A Math. Phys. Eng. Sci. **115(772)** (1927), 700–721.

[55] M. Khalil, A. Am Arafa, and A. Sayed, *A variable fractional order network model of Zika virus*, J. Fract. Calc. Appl. **9(1)** (2018), 204–221.

[56] M.A. Khan, S.W. Shah, S. Ullah, and J.F. Gómez-Aguilar, *A dynamical model of asymptomatic carrier Zika virus with optimal control strategies*, Nonlinear Analysis: Real World Appl. **50** (2019), 144–170.

[57] M.A. Khan, S. Ullah, and M. Farhan, *The dynamics of Zika virus with Caputo fractional derivative*, AIMS Math. **4(1)** (2019), 134–146.

[58] M.A. Khan, M. Ismail, S. Ullah, and M. Farhan, *Fractional order SIR model with generalized incidence rate*, AIMS Math. **5(3)** (2020), 1856–1880.

[59] A.J. Kucharski, S. Funk, R.M. Eggo, H.-P. Mallet, W.J. Edmunds, and E.J. Nilles, *Transmission dynamics of Zika virus in island populations: a modelling analysis of the 2013/14 French Polynesia outbreak*, PLoS neglected Tropical Diseases **10(5)** (2016): e0004726.

[60] L. Lambrechts, *Impact of daily temperature fluctuations on Dengue virus transmission by Aedes Aegypti*, Proc. Natl. Acad. Sci. USA **108(1)** (2011), 7460–7465.

[61] E.K. Lee, Y. Liu, and F.H. Pietz, *A compartmental model for Zika virus with dynamic human and vector populations*, AMIA Annu. Symp. Proc. **2016** (2011), 743–752.

[62] B. Li, T. Wang, and X. Xie, *Analysis of the L1 scheme for fractional wave equations with nonsmooth data*, Comput. Math. Appl. **90** (2021), 1–12.

[63] V.M.C. Lormeau, *Zika virus, French Polynesia, South Pacific*, Emerg. Infect. Dis. **20(6)** (2014), 1085–1086.

[64] M.H. Maamar, L. Bouzid, O. Belhamiti, and F.B.M. Belgacem, *Stability and numerical study of theoretical model of Zika virus transmission*, Int. J. Math. Modell. Numer. Optim. **10(2)** (2020), 141–166.

[65] R.W. Malone, J. Homan, M.V. Callahan, et al., *Zika virus: medical countermeasure development challenges*, PLoS Negl. Trop. Dis. **10(3)** (2016), e0004530.

[66] C. Manore and M. Hyman, *Mathematical models for fighting Zika virus*, SIAM News **49(4)** (2016), 1.

[67] C.A. Manore, R.S. Ostfeld, F.B. Agusto, H. Gaff, and S.L. LaDeau, *Defining the risk of Zika and Chikungunya virus transmission in human population centers of the eastern United States*, PLoS Neglected Tropical Diseases **11(1)** (2017), e0005255.

[68] M. Martcheva, *An Introduction to Mathematical Epidemiology*, Springer, New York, 2015.

[69] D. Matignon, *Stability results for fractional differential equations with applications to control processing*, Comput. Eng. Syst. Appl **2** (1996), 963–968.

[70] P.S. Mead, S.L. Hills, and J.T. Brooks, *Zika virus as a sexually transmitted pathogen*, Current Opinion in Infectious Diseases **31(1)** (2018), 39–44.

[71] M.M. Khalsaraei, *Positivity of an explicit Runge–Kutta method*, Ain Shams Engrg. J. **6(4)** (2015), 1217–1223.

[72] J.P. Messina, *Mapping global environmental suitability for Zika virus*, elife **5** (2016), e15272.

[73] R.E. Mickens, *Applications of Nonstandard Finite Difference Schemes*, World Scientific, 2000.

[74] R.E. Mickens, *Calculation of denominator functions for nonstandard finite difference schemes for differential equations satisfying a positivity condition*, Numer. Meth. Part. Diff. Eqs. **23(3)** (2007), 672–691.

[75] A.A. Momoh and A. Fügenschuh, *Optimal control of intervention strategies and cost effectiveness analysis for a Zika virus model*, Oper. Res. Health Care **18** (2018) 99–111.

[76] S.C. Mpeshe, N. Nyerere, and S. Sanga, *Modeling approach to investigate the dynamics of Zika virus fever: A neglected disease in Africa*, Int. J. Adv. Appl. Math. Mech. **4(3)** (2017) 14–21.

[77] D. Musso and D.J. Gubler, *Zika virus: following the path of Dengue and Chikungunya?*, Lancet **386(9990)** (2015), 243–244.

[78] D. Musso and D.J. Gubler, *Zika virus*, Clin. Microbiol. Rev. **29(3)** (2016), 487–524.

[79] P.A. Naik, *Global dynamics of a fractional-order SIR epidemic model with memory*, Int. J. Biomath. **13(8)** (2020), 2050071.

[80] P.A. Naik, M. Yavuz, and J. Zu, *The role of prostitution on HIV transmission with memory: A modeling approach*, Alexandria Engrg. J. **59(4)** (2020), 2513–2531.

[81] H. Nishiura, R. Kinoshita, K. Mizumoto, Y. Yasuda, and K. Nah, *Transmission potential of Zika virus infection in the south pacific*, Int. J. Infect. Dis. **45** (2016), 95–97.

[82] E. Okyere, S. Olaniyi, and E. Bonyah, *Analysis of Zika virus dynamics with sexual transmission route using multiple optimal controls*, Scientific African **9** (2020), e00532.

[83] S.J.A.M. Olaniyi, *Dynamics of Zika virus model with nonlinear incidence and optimal control strategies*, Appl. Math. Inf. Sci. **12(5)** (2018), 969–982.

[84] PAHO/WHO from Brazil, *International Health Regulation (IHR)*, National Focal Point (NFP), PAHO/WHO, 2 March, 2017.

[85] T.A. Perkins, A.S. Siraj, C.W. Ruktanonchai, M.U. Kraemer, and A.J. Tatem, *Model-based projections of Zika virus infections in childbearing women in the Americas*, Nat. Microbiol. **1(9)** (2016), 16126.

[86] I. Podlubny, *Fractional Differential Equations: An Introduction to Fractional Derivatives, Fractional Differential Equations, to Methods of their Solution and some of their Applications*, Elsevier, 1998.
[87] R. Prasad, K. Kumar, and R. Dohare, *Caputo fractional order derivative model of Zika virus transmission dynamics*, J. Math. Comput. Sci. **2023(28)** (2023), 145–157.
[88] S. Qureshi and R. Jan, *Modeling of measles epidemic with optimized fractional order under Caputo differential operator*, Chaos, Solitons & Fractals **145** (2021), 110766.
[89] R. Rakkiyappan, V.P. Latha, and F.A. Rihan, *A fractional-order model for Zika virus infection with multiple delays*, Complexity, 2019.
[90] S. Rezapour, H. Mohammadi, and M.E. Samei, *SEIR epidemic model for COVID-19 transmission by Caputo derivative of fractional order*, Adv. Diff. Eqs. **2020(1)** (2020), 1–19.
[91] S. Rezapour, H. Mohammadi, and A. Jajarmi, *A new mathematical model for Zika virus transmission*, Adv. Diff. Eqs. 2020(1) (2020), 1–15.
[92] R.G. Sargent, *Verification and validation of simulation models*, J. Simul. **7(1)** (2013), 12–24.
[93] T.W. Scott, *Longitudinal studies of Aedes Aegypti (Diptera: Culicidae) in Thailand and Puerto Rico: blood feeding frequency*, J. Med. Entomol. **37(1)** (2000), 89–101.
[94] P. Shapshak, *Global Virology I – Identifying and Investigating Viral Diseases*, Springer, New York, 2015.
[95] A. Sherly and W. Bock, *Multipatch ZIKV Model and Simulations*, in: M. Ehrhardt and M. Günther (eds.), Progress in Industrial Mathematics at ECMI 2021, The European Consortium for Mathematics in Industry 39, Springer, 2022.
[96] M. Stynes, *A survey of the L1 scheme in the discretisation of time-fractional problems*, Preprint January 2021.
[97] M.A. Taneco-Hernández and C. Vargas-De-León, *Stability and Lyapunov functions for systems with Atangana-Baleanu Caputo derivative: an HIV/AIDS epidemic model*, Chaos, Solitons & Fractals **132** (2020), 109586.
[98] Y.A. Terefe, H. Gaff, M. Kamga, and L. van der Mescht, *Mathematics of a model for Zika transmission dynamics*, Theory Biosci. **137(2)** (2018) 209–218.
[99] J. Tolles and T.B. Long, *Modeling epidemics with compartmental models*, JAMA Guide Stat. Meth. **323(24)** (2020), 2515–2516.
[100] S. Treibert, H. Brunner, and M. Ehrhardt, *A nonstandard finite difference scheme for the SVICDR model to predict COVID-19 dynamics*, Math. Biosci. Engrg **19(2)** (2022), 1213–1238.
[101] D. Wang, A. Xiao, and J. Zou, *Long-time behavior of numerical solutions to nonlinear fractional ODEs*. ESAIM: Math. Modell. Numer. Anal. 54(1) (2020), 335–358.
[102] D. Wang and J. Zou, *Mittag–Leffler stability of numerical solutions to time fractional ODEs*, Numerical Algorithms (2022), 1–35.
[103] F.L.H. Wertheim, P. Horby, and J.P. Woodall, *Atlas of Human Infectious Diseases*, Wiley-Blackwell, Oxford, 2012.
[104] Y. Xing and Y. Yan, *A higher order numerical method for time fractional partial differential equations with nonsmooth data*, J. Comput. Phys. **357** (2018), 305–323.
[105] Y. Yan, M. Khan, and N.J. Ford, *An analysis of the modified L1 scheme for time-fractional partial differential equations with nonsmooth data*, SIAM J. Numer. Anal. **56(1)** (2018), 210–227.
[106] C. Zanluca, *First report of autochthonous transmission of Zika virus in Brazil*, Inst. Oswaldo Cruz. **110(4)** (2015), 569–572.

Department of Mathematics and Computer Science, Abdelhamid Ibn Badis University, Algeria
Email address: `maghnia.hamoumaamar@gmail.com`

Chair of Applied and Computational Mathematics, University of Wuppertal, Germany
Email address: `ehrhardt@uni-wuppertal.de`

Department of Mathematics and Computer Science, Abdelhamid Ibn Badis University, Algeria
Email address: `louiza.tabharit@univ-mosta.dz`